THE BELL SYSTEM TECHNICAL JOURNAL
Vol. 57, No. 7, September 1978
Printed in U.S.A.

SG Undersea Cable System:

Repeater and Equalizer Design and Manufacture

By C. D. ANDERSON, W. E. HOWER, J. J. KASSIG, V. M. KRYGOWSKI, R. L. LYNCH, G. A. REINOLD, and P. A. YEISLEY

(Manuscript received May 30, 1978)

Linearity and reproducibility of undersea electronics play key roles in determining the achievable performance of an undersea cable system. This paper describes the characteristics of undersea electronics and the measures taken in design and manufacture to achieve the desired performance and reliability, giving special emphasis to new features and applications. It describes in detail the performance achieved in the recently completed SG system linking the U.S. and France.

I. INTRODUCTION

Exploratory work on undersea amplifiers and devices in the late 1960s produced models of repeaters with the performance required for a 3500-channel, 4000-nmi system with a top frequency of 27.5 MHz. The specific development of the 30-MHz, 4000-channel, SG system was started early in 1971. The first SG installation, TAT-6, which connects Green Hill, R.I., with St. Hilaire, France, was completed in July 1976, yielding 4200 channels.

The fivefold increase in bandwidth of SG over SF[1] was made technically possible by advances in the design of reliable, ultralinear, silicon microwave transistors.[6] Manufacturing the necessary numbers of undersea bodies economically and on schedule required substantial innovations in the basic mechanical construction and assembly techniques of the electronic units.

II. GENERAL OBJECTIVES

2.1 Noise and load

The SG system was designed to meet the international objectives of 1 pWp0/km (38.6 dBrnc0 for 3500 nmi), average, with a signal load of −13 dBm0 per 3-kHz spaced channel. The "worst channel" could be 2 pWp0/km. Once the noise, load, channel capacity, and cable diameter are specified, and the achievable amplifier noise figure and modulation coefficients are known, the repeater gain (and spacing) can be determined from the following approximate relationship:

$$\text{s/n} = -1.8 - \frac{1}{3}\left[M_{A+B-C} + 10\log(\overline{n_p}) + 20\log(n)\right] - \frac{2}{3}\left[10\log(KTB) + N_F + G_R + 10\log(n)\right], \quad (1)$$

where

s/n = signal-to-noise ratio in decibels,
M_{A+B-C} = repeater third-order modulation coefficient for 3-tone products of the $A + B - C$ type (−95.0 dBm),
n = number of repeaters in the system (690),
$\overline{n_p}$ = equivalent number of third-order intermodulation products which add in phase from repeater to repeater (376,000),
KTB = thermal noise = −139 dBm at 300°K in 3 kHz,
N_F = repeater noise figure (3.5 dB),
G_R = repeater insertion gain (41.0 dB).

The numbers in parentheses indicate the approximate 29.5-MHz values. The channel noise and load objectives (38.6 dBrnc0 and −13 dBm0, respectively) translate to a system s/n ratio of 36.4 dB. Equation (1) evaluated at 29.5 MHz yields an s/n ratio of 36.4 dB. More detailed analysis showed that proper signal level shaping would significantly reduce the noise at lower frequencies. It thus appeared that we could meet the noise objectives.

2.2 Transmission

Because optimum repeater noise performance can be obtained only over a narrow range of signal power, it is necessary to accurately match the repeater gain to the cable section loss. The errors between the two are compensated for in the ocean-block equalizers (OBEs) which follow every 20 or 30 repeaters. The allocation of repeater, equalizer, and cable loss deviations are detailed in another article.[2] For a 20-repeater block (TAT-6), the top frequency loss deviation allowances are ±0.03-dB systematic and ±0.1 dB random for repeaters and ±0.1 dB total for OBEs.

The deviation allocations are increased at lower frequencies up to a maximum of $1\frac{1}{2}$ times the top-frequency value, in proportion to $30/f$, where f is in MHz.

Available gain for the equalizers is obtained by reducing the length of cable by 4.1 nmi, that is, from 5.1 nmi for repeater sections to 1.0 nmi for equalizer sections. Additional low-frequency gain range is derived from a repeater gain boost of the form:

$$\begin{aligned} \text{repeater gain boost (dB)} &= 0.00218(11.5\text{-}f)^2 \quad f \leq 11.5 \\ &= 0 \qquad\qquad\qquad\quad f > 11.5, \end{aligned} \tag{2}$$

where f is in MHz.

Cable loss variations due to the seasonal temperature changes on the continental shelves are equalized by temperature-controlled repeaters. The gain of these repeaters is controlled by an ambient-temperature-sensing thermistor in the amplifier feedback circuit. The objective was to equalize at least $\frac{2}{3}$ of the shallow-water loss variation, leaving only a smooth residual which could be readily equalized in the terminals.

To meet noise objectives over the 20-year minimum life of the system requires means of equalizing any reasonably likely transmission change which occurs during that period. Shore-controlled equalizers (SCEs) were introduced when cable "aging" (change in attenuation with time) was predicted to be of serious consequence.[3] Each SCE has a controllable loss range of ±16 dB at 30 MHz with 2-dB step sizes.

2.3 Mechanical

To ensure that the repeaters and equalizers survive the shocks associated with laying and recovery, they are designed to withstand:

(*i*) A 60-g shock peak for 60-ms duration between half-amplitude points along each of the three principal axes.
(*ii*) A vibration limit of 1.27-cm sinusoidal peak-to-peak displacement from 5 to 11 Hz.
(*iii*) A sinusoidal vibration at 3-g maximum from 11 to 500 Hz.

The underwater electronics are designed to operate over a temperature range of 0° to 30°C (32° to 86°F). The allowable storage temperature range is: −18° to 57°C (0° to 135°F).

The maximum permissible leak rate of a sealed pressure housing under helium pressure test is 1×10^{-7} standard cc/s at 844 kg/cm^2 (12,000 psi). This is the pressure at a depth of 8050 m (26,000 ft). Individual components such as seals are allowed a maximum leak rate of 5×10^{-8} standard cc/s.

Table I — New materials, processes, and techniques

Materials	
Aluminum	AA 356.0 and AA-6061
Bronze	CA-725
Thermoplastic	Glass-reinformed polybutylene terephthalate (PBT)
Stainless steel	Types 305, 310, and 384

Processes	Techniques
Back extrusion	Printed-wiring boards
Electron beam welding	Vacuum drying
Low-pressure permanent-mold castings	

III. MECHANICAL DESIGN

3.1 New techniques

The physical design of the SG underwater hardware (Fig. 1) embodies some principles proven in the past and some which are new to undersea use. Those materials, processes, and techniques newly exploited in undersea cable use are listed in Table I.

3.2 Pressure hull

The cylindrical copper beryllium housing is back-extruded rather than forward-extruded. This change has led to a housing which costs about the same as those used for the earlier SD and SF systems in current dollars. The back-extruded housing more than satisfies the corrosion resistance, grain size, porosity, and strength requirements.

The tungsten inert gas (TIG) method of welding the cover to the housing has been replaced by electron beam (eB) welding. A high-intensity (about 1.4 MW/cm^2) stream of electrons is focused to a controlled beam size upon the weld seam in a vacuum. The kinetic energy of the beam is converted into heat upon impact with the copper beryllium, causing it to melt, vaporize, and then condense on the cooled material surrounding the melt trough. The weld progresses continuously as the cover and housing rotate under the beam.

The weld depth and melt zone geometry have been optimized for minimum stress by rigidly controlling the beam current, diameter, accelerating voltage, focal distance, work distance, and welding speed. Weld depths are typically 3.8 mm. In the rare case of a process or apparatus failure during assembly, the eB process permits up to two repair welds. Such a failure with the TIG process required a machining operation which destroyed either housing or cover.

3.3 Electronics unit

The most significant departure from previous practice was the elimination of hermetic sealing of the electronics block of the repeater and equalizer units. Analyses had shown that by taking advantage of the

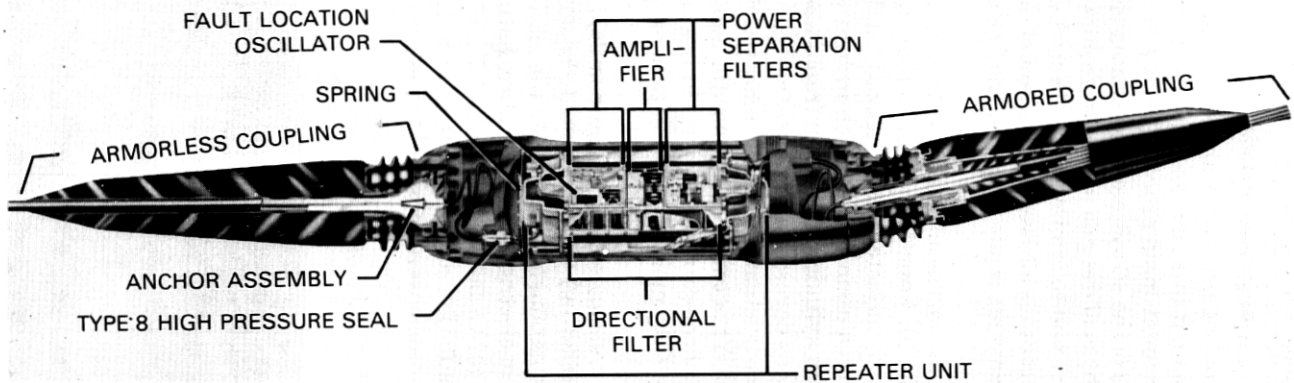

Fig. 1—SG repeater.

water absorption properties of the plastic materials within the electronics unit, the inner assembly (Fig. 2) can be left open inside the pressure housing without danger of moisture condensation. This greatly simplified the design of the inner unit. It allowed the cylinder to be extruded, which simplified the epoxy coating procedure and subsequent assembly with the main frame. The main frame and associated structures were cast by the low-pressure permanent-mold process (LPPM).

The frequency range of the SG system necessitated close coordination of the electrical and physical designs of the electronics units to achieve the needed performance and to minimize unit-to-unit variations. In the repeater, assembly procedures allowed adjustment of over 30 inductors. Five of these adjustments are made after final assembly of all the networks.

Each individual circuit was mounted on its own aluminum frame as a separate module (Fig. 3). Functional partitioning allowed networks to be assembled, tested, adjusted, and "locked" individually. Each module was mounted on a main frame which in turn was slid into the epoxy-coated aluminum cylinder. The main frame was then locked to the cylinder and the ends covered with plastic end caps.

The modular type construction using cast frames provided low thermal impedance (about 1°C/W) between the transistor mounting studs and the housing. This type of construction also minimizes corona due to the high voltages (up to 7 kV) by maintaining isolation, proper spacing, and smooth surfaces.

Glass epoxy double- and single-sided circuit boards, 1.588 mm (0.0625 in.) and 2.381 mm (0.0935 in.) thick, supplied the structural rigidity needed for mounting components and highly repeatable circuit paths to minimize variations in electrical characteristics. Path widths were set at 2.54 mm (0.100 in.) with a minimum spacing of 1.27 mm (0.050 in.). Dielectric constant, insulation resistance, peel strength, plating thickness, and breakdown voltage were required to meet stringent limits to insure high reliability.

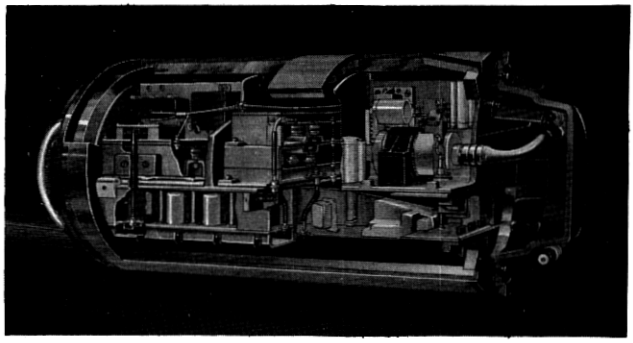

Fig. 2—Electronics unit, inner assembly.

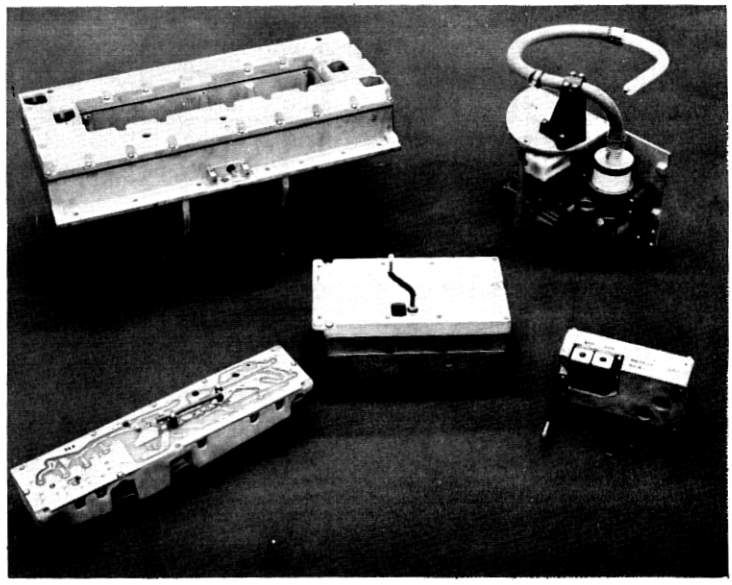

Fig. 3—Circuit modules. Top left, directional filter (DF); top right, ground separation filter (GSF); bottom left, output network; center, amplifier; bottom right, oscillator.

Because of the high potential of the electronic units, it was desirable to make the end caps from insulating material. A glass-filled polybutylene terephthalate (PBT) was selected because of its excellent mechanical and electrical properties. In addition, its low shrink factor and good flow characteristics make it a good material for injection molding. PBT has a melting temperature greater than 216°C (420°F) and therefore allows for soldering on or near its surface. The material has also been used for electrical standoffs and insulating covers.

Although the decision to use a nonhermetically sealed electronics unit permitted the exploitation of new materials and processes, it required a new vacuum drying procedure which considered the outgassing and water absorption properties of all the materials in the unit. A drying cycle and a closure procedure have been devised which predict a dew point of less than −15°C (+5°F) after 20 years at sea bottom at an external pressure of 844 kg/cm^2 (12,000 psi).

IV. REPEATER ELECTRICAL DESIGN

4.1 Configuration

As described in a companion article,[2] the repeater gain is provided by a pair of tandem amplifiers common to both transmission bands.

Table II contains a summary of the repeater electrical performance.

Table II — SG repeater electrical performance summary

Frequency (mHz)	Repeater Gain (dB)	Amplifier Gain (dB)	Network Losses (dB)	Repeater Noise Figure (dB)	Modulation Coefficients* M_{2E}* (dB)	Modulation Coefficients* M_{3E}* (dB)	Repeater Return Loss A end (dB)	Repeater Return Loss B end (dB)
1	7.48	10.56	3.08	8.7	−112	†	34	25
2	10.37	12.13	1.76	8.0	−116	†	36	24
4	14.53	15.94	1.41	7.7	−110	†	33	22
8	20.50	22.07	1.57	7.0	−100	†	25	30
12	25.34	27.67	2.33	5.8	−84	†	22	17
13.75	27.20	30.64	3.44	5.8	−79	†	22	22
16.50	29.96	33.00	3.04	5.2	−77	−113	27	19
20	33.23	34.99	1.76	4.0	−73	−113	24	26
25	37.46	39.09	1.63	3.6	−71	−113	21	23
30	41.37	42.89	1.52	3.5	−70	−113	24	20

* Defined at power amplifier output. The value of M_{3E} is that determined before installation of TAT-6. As discussed later in Section VII, this value is better than the actual repeater performance.

† M_{3E} is not a significant parameter in the low band.

4.2 Passive networks

4.2.1 Ground-separation filter

The ground-separation filters (GSFs) shown in Fig. 4 connect the cable to the directional filters. They were designed as high-pass filters. Coaxial capacitors (0.013 μF) provide a low-impedance ground path for signal frequencies, while blocking the high dc voltage (up to 7 kV) which exists between the repeater unit (repeater ground) and the housing (sea ground). To prevent coupling between the repeater input and output, this impedance should ideally be zero. However, at low frequencies the reactance of the high-voltage capacitor becomes large, while at high frequencies inductive parasites dominate. The coaxial design virtually eliminates the inductance problem in the capacitor. A coaxial choke with a longitudinal inductance of 250 μH reduces the unbalanced current in the GSF and thereby increases the isolation between the repeater input and output. Adequate GSF loop loss* was achieved without building up the capacitance between the inner unit and the housing.

Powder core inductors carry the 657-mA dc line current to the amplifier biasing circuits. Each inductor along with the adjacent 0.013-μF coaxial and low-voltage ceramic capacitors forms a full-section, 50-ohm, high-pass filter with a cutoff frequency of about 300 kHz.

4.2.2 Directional filters

The directional filter is a 50-ohm, four-port network with two high-pass and two low-pass filters. They are of conventional design using oppositely phased transformers in the two low-pass portions to help

* GSF loop loss refers to stray transmission around the amplifier via the GSFs and the repeater's power path.

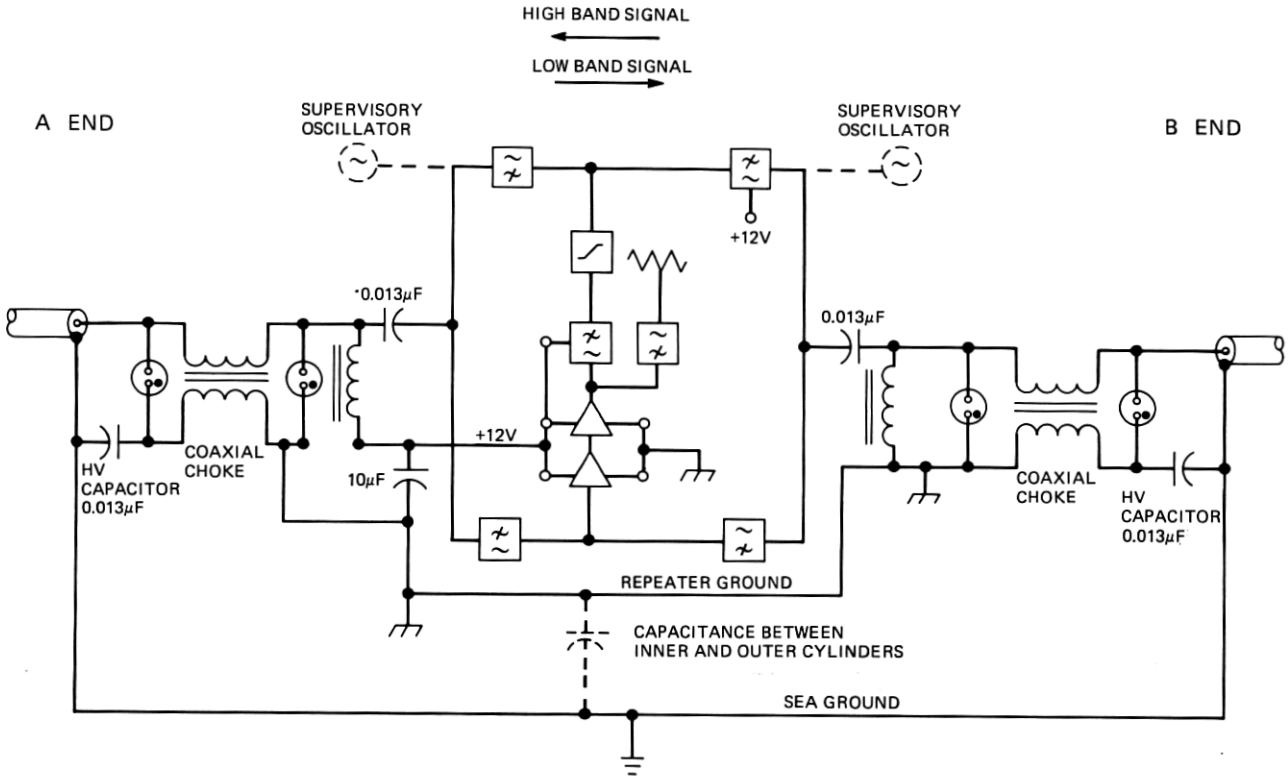

Fig. 4—SG repeater block diagram showing GSF circuit.

increase directional filter loop loss.† Figure 5 shows the rectangular arrangement and the individual shielded inductor compartments that provide ideal isolation between both sections and ports. All components are mounted on a single board and connected with printed wiring. The individual sections are tuned "in place" after all filter wiring is complete.

4.2.3 Output network

The output network, shown in Fig. 6, contains surge protection diodes, a low-pass bandlimiting filter, a low-frequency loss equalizer, and a high-pass terminating filter. The filter pair was designed on a constant-R basis with a 3-dB crossover at 33.5 MHz. The low-pass filter increases the high-frequency loop loss around the amplifier and improves the noise sing margin[4] by suppressing the transmission of above-band noise. The high-pass section properly terminates the power amplifier at high frequencies, thereby maintaining a uniform and controlled stability margin.

A constant-R bridged-T equalizing network helps shape the repeater

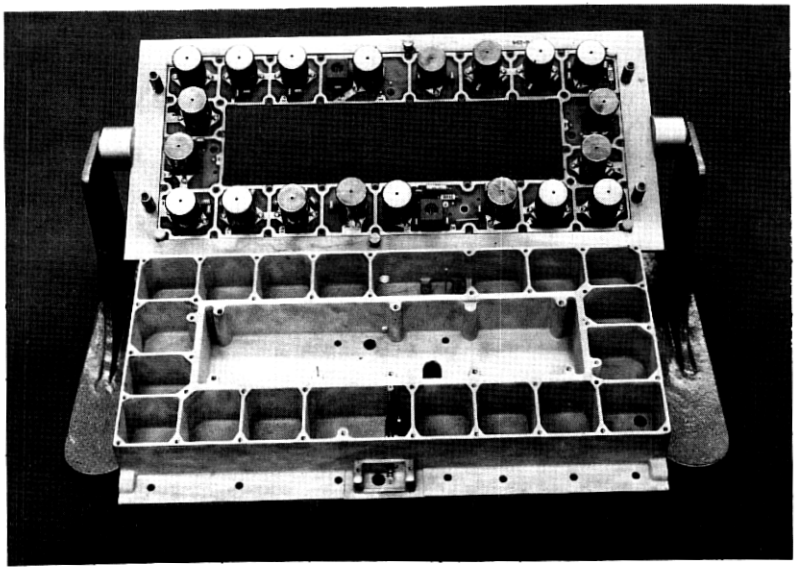

Fig. 5—Directional filter.

† Directional filter loop loss refers to the stray transmission around the amplifier via the tandem-paired filters, both high pass/low pass and low pass/high pass. Providing a phase reversal in one of the two paths increases the total loss because transmission via one path tends to cancel that via the other.

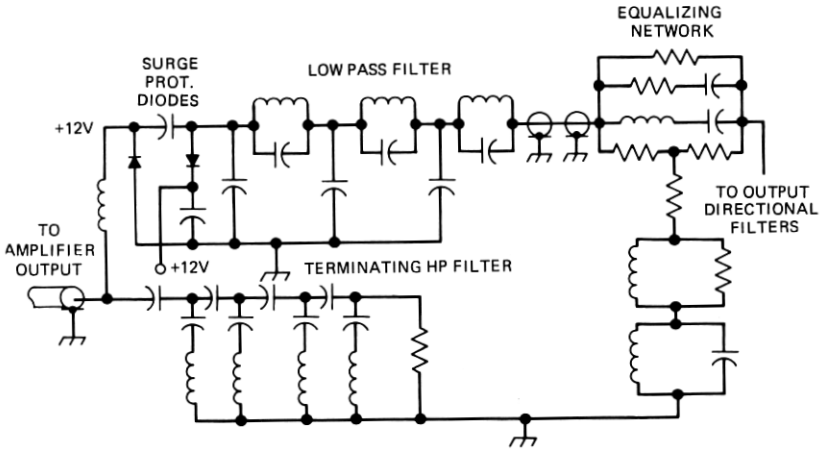

Fig. 6—Output network schematic.

gain and increases the output return loss and the external loop loss at low frequencies.

A pair of oppositely poled, reverse-biased diodes, whose capacitance is absorbed in the low-pass filter, provides surge protection for the power amplifier.

4.3 Amplifier

4.3.1 Configuration

The amplifier (Fig. 7) consists of a two-stage preamplifier (PRA) and a three-stage power amplifier (PWA). Both PRA stages are common emitter while the PWA uses a common-base output stage, driven from a Darlington pair via a current step-up transformer. The gain is shaped with feedback. Shunt input, series output is used in the PRA, and shunt input, shunt output in the PWA. Feedback with hybrid-connected autotransformers actively terminate the amplifier input and output ports. The PRA, which has a high output impedance, is connected to the low-input impedance PWA with a resistor. This arrangement reduces the impedance interaction effect between the two at their respective loop gain and phase crossover frequencies and minimizes stability problems.

4.3.2 Bias

The repeaters are biased at 657 ± 0.3 mA with an average voltage of 11.9 V (at 2.5°C). Nominal operating points of individual transistors are listed in Table III. The input stage of the PRA is biased from the emitter of the second stage. During power turn-up, the first stage does not begin to conduct until the second-stage current reaches about 50 mA.

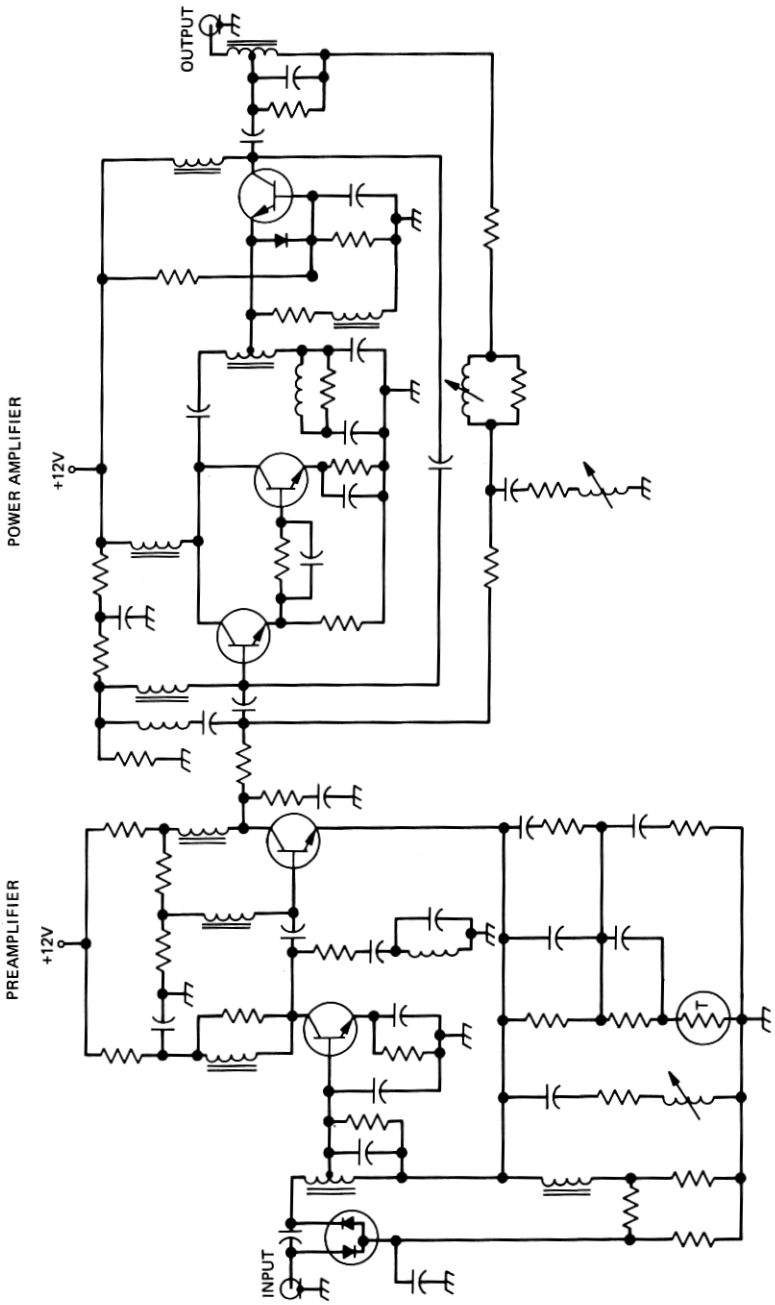

Fig. 7—SG amplifier schematic.

Table III — Nominal transistor operating points (2.5°C)

	Stage	Collector-Emitter Voltage (V)	Collector Current (mA)
Preamplifier	1	9.44	49.8
	2	9.24	153.1
Power amplifier	3	9.16	50.2
	4	10.05	147.2
	5	9.99	147.2
Oscillator		8.05	9.2
Subtotal			556.7
Bleeder current (mA)			100.3
Total (mA)			657.0

Staggering the currents at which the two stages begin to develop gain avoids oscillation which can occur during power turn-on of feedback amplifiers. The dc-coupled Darlington pair in the PWA operates similarly.

4.3.3 Gain

The amplifier gain objective equals the sum of:

(*i*) The loss of 5.1 nmi of cable at 2.5°C, 2.5 kilofathoms.
(*ii*) The loss of the repeater passive networks.
(*iii*) The low-band gain boost.

The amplifier gain, 43 dB at 30 MHz, is divided approximately equally between the PRA and the PWA. It is controlled by the feedback circuits in both amplifiers. The repeater gain, which is further shaped by the bridged-T equalizer in the output network, was initially matched to within +0.03 dB of the objective.* This necessitated extensive characterization of each component and the printed wiring boards. Component tolerances were assigned based upon both sensitivity studies and adjustment capability. The amplifier contains three adjustable inductors. Two are adjusted during the final repeater network testing stage along with an inductor in the output network and two in the directional filters.†

The shapes obtained with these final adjustments closely match the shapes of the three most significant sources of gain deviation:

(*i*) Directional filter and output network loss variations.
(*ii*) Miller capacitance of Darlington pair.
(*iii*) Alpha sensitivity of the second stage in the Darlington pair.

The effectiveness of the gain control and adjustment techniques is

* The low-frequency gain was later increased slightly to obtain more channels below 1 MHz at the expense of increasing the low-frequency gain deviation somewhat.

† This operation is discussed in Section 6.3.5.

indicated in Table IV, which is based upon the entire TAT-6 repeater production.

There are two basic types of SG amplifiers, fixed-gain and temperature controlled (TC). The latter, which are new to undersea cables, are used in those repeaters to be laid in shallow water areas where bottom temperatures change seasonally. The gain of TC repeaters is designed to increase with temperature, as does cable loss. Gain is controlled by an ambient temperature-sensing parallel-disk thermistor in the PRA feedback circuit. Figure 8 shows the repeater gain and the cable-loss change for a temperature rise from 2.5° to 10.1°C. Over this range, the repeater compensates for at least $\frac{2}{3}$ of the cable loss change. The TC repeater is designed to have the same gain at 2.5°C as the fixed-gain repeater.

4.3.4 Feedback

The achievable feedback is limited by both conventional and noise-sing stability considerations. As shown in Fig. 9, the nominal PRA feed-

Table IV — Repeater gain objective and average* deviation (dB) at 2.5°C

Low Band				High Band			
Freq (MHz)	dB Gain Objective	Deviation without Termina-tions	Deviation† with Termina-tions	Freq (MHz)	dB Gain Objective	Deviation without Termina-tions	Deviation† with Termina-tions
0.75	6.404	−0.018	−0.018	16.50	29.950	−0.006	−0.017
1.00	7.346	0.092	0.092	16.75	30.190	0.001	0.026
1.50	8.935	0.094	0.094	17.00	30.430	−0.006	0.026
2.00	10.281	0.060	0.060	17.25	30.667	−0.005	0.026
2.50	11.469	0.044	0.044	17.50	30.904	−0.001	0.025
3.00	12.546	0.036	0.036	17.75	31.138	0.008	0.023
3.50	13.540	0.032	0.032	18.00	31.373	0.015	0.010
4.00	14.470	0.037	0.036	18.50	31.835	0.027	0.002
5.00	16.176	0.027	0.029	19.00	32.293	0.027	0.002
6.00	17.730	0.007	0.010	19.50	32.745	0.026	0.012
7.00	19.170	−0.019	−0.020	20.00	33.193	0.020	0.020
8.00	20.520	−0.047	−0.051	21.00	34.075	0.008	0.016
9.00	21.797	−0.063	−0.057	22.00	34.940	0.001	0.008
10.00	23.015	−0.044	0.046	23.00	35.788	−0.002	0.006
10.50	23.604	−0.030	−0.028	24.00	36.622	−0.007	0.006
11.00	24.182	−0.018	−0.019	25.00	37.441	−0.006	−0.003
11.50	24.751	−0.009	−0.003	26.00	38.248	−0.002	−0.029
12.00	25.309	−0.001	−0.014	27.00	39.042	0.008	−0.032
12.50	25.859	−0.009	−0.003	27.50	39.435	0.012	0.024
12.75	26.130	−0.015	−0.020	28.00	39.824	0.018	−0.001
13.00	26.398	−0.015	−0.030	28.50	40.211	0.023	0.026
13.25	26.665	−0.013	−0.024	29.00	40.596	0.024	0.045
13.50	26.929	−0.007	−0.007	29.50	40.978	0.016	0.048
13.75	27.192	0.001	0.009	30.00	41.357	−0.013	0.012

* Based upon all the TAT-6 repeaters.
† Refers to armorless terminations.

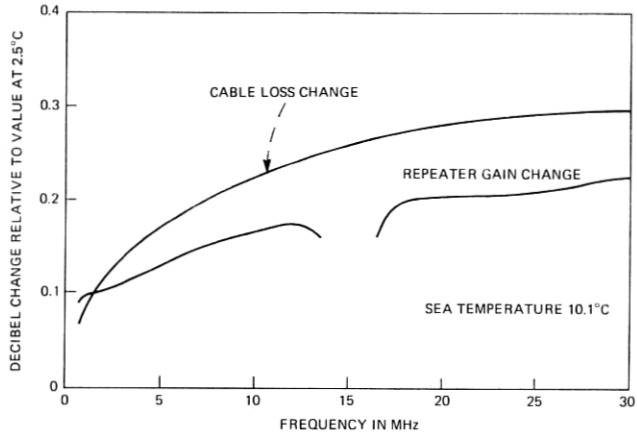

Fig. 8—Gain tracking of temperature-controlled repeater.

back ranges from 32 dB at 5 MHz to 11 dB at 30 MHz, while the PWA feedback is maximum at 1.5 MHz and decreases to 12 dB at 30 MHz. The repeater is stable for all combinations of open and short circuit terminations, for all possible combinations of transistors up to at least 45°C and at reduced currents, which occur during power turn-up. The

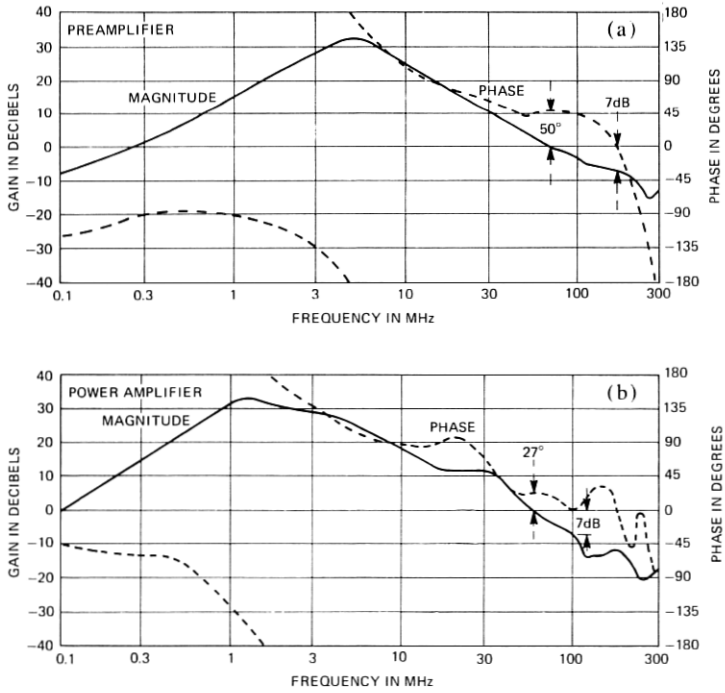

Fig. 9—Amplifier feedback.

noise-sing margin of the system is strongly influenced by the phase of both the inband and aboveband loop feedback of the PWA. Maintaining the phase characteristics near 90° across the high band and as large as possible aboveband resulted in significant improvement in the noise-sing margin.

4.3.5 Thermal noise and intermodulation distortion

The nominal repeater noise figure and intermodulation coefficients are shown in Table II. A 30-MHz noise figure of 3.5 dB was achieved by using a low-loss active termination and by selecting low noise-figure transistors for the input stage.

Second-order distortion coefficients range from −70 dBm at 30 MHz to −112 dBm at 1 MHz. The tandem amplifier configuration results in some fundamental frequency dependence in the coefficients. Because of the shaped gain in both amplifiers, the PRA second-order distortion contribution is significant for low-frequency fundamentals.

Third-order distortion products of the $A + B - C$ type are the most important because of their number and their tendency to add in-phase from repeater to repeater. Measurements of many different products of this type during development and manufacture of the SG repeater indicated a value for M_{3E} of approximately −113 dB in the high band.* As discussed further in Section 7.2, the characterization of third-order distortion was misleading because a source of distortion existed that did not obey the usual rules.

4.3.6 Overload protection

Reverse current flow across the emitter-base junction of a silicon planar transistor can cause a change in the current gain. Although these junctions are forward-biased in the amplifier, abnormally large signal voltages can, in the output stage, produce voltages in the emitter-base breakdown region. Such abnormal signals can result from certain failures in the terminal equipment, or in the land facilities feeding the system, or from improper test procedures. The output stage of the PWA is protected against signal overload by a diode connected across the emitter-base junction. Additional protection is provided in the shore terminals.[5]

4.4 Supervisory oscillator

A single-transistor, crystal-controlled oscillator injects a unique frequency at the input of each repeater. These supervisory tones, which fall

* Defined at amplifier output.

alternately in the high and low bands, are used for monitoring transmission levels and localizing faults on the system. A diode limiter and a thermistor-controlled attenuator maintain a stable tone power at the repeater output of −50 and −40 dBm in the low and high bands, respectively. The quartz crystals are circular, plano-convex, AT cut. They resonate in the fifth overtone thickness shear mode. Crystal characteristics are listed in Table V.

4.5 Transistors

The 82-type transistor[6] used in the SG amplifier features a common design for all stages. It is a silicon planar epitaxial type with an f_T of 2.7 GHz designed to operate for 20 years at 1.5 W and a maximum junction temperature of 65°C with a maximum α_0 change of 0.0005. (Sample aging measurements to date indicate no discernible aging.)

Each transistor's small signal characteristics were determined at 10 V, 150 mA, and 9 V, 50 mA, the two nominal operating points. Two-port transmission parameters at 15 frequencies from 100 kHz to 400 MHz were computer-processed by an "on-line" circuit-modeling program to yield element values in the equivalent circuit of Fig. 10. Thus, each set of 60 complex transmission parameters was reduced to nine circuit elements. Noise figure and intermodulation coefficients at the two bias points were also measured. A transistor assignment program optimized the usage of a given lot of transistors by assigning each transistor to a stage in the repeater on the basis of its so-called "noise numbers." Five noise numbers were computed for each transistor. These numbers were proportional to the system noise which would be contributed by the transistor in each possible use.

The input stage noise number was proportional to the 30-MHz noise figure, while the output-stage noise number was dominated by the transistor third-order modulation coefficient. The program minimized the sum of the noise numbers, while yielding a required number of complete transistor sets. There were no grouping requirements based upon stability or gain deviation considerations. Table VI lists the median ac parameters of all transistors used in the TAT-6 link.

Table V — Crystal characteristics

	Low Band	High Band
Frequency band (MHz)	11.120–11.216	27.628–27.820
Spacing between tones (Hz)	200	400
Accuracy from nominal (Hz) (over 20 years and 0° to 45°C)	−118, +40	−293, +98
Resistance-min-max (ohms)	20–100	10–50
Shunt capacitance (pF)	4.25	8.4
Inductance (mH)	500	40
Q	350K to 1750K	140K to 700K

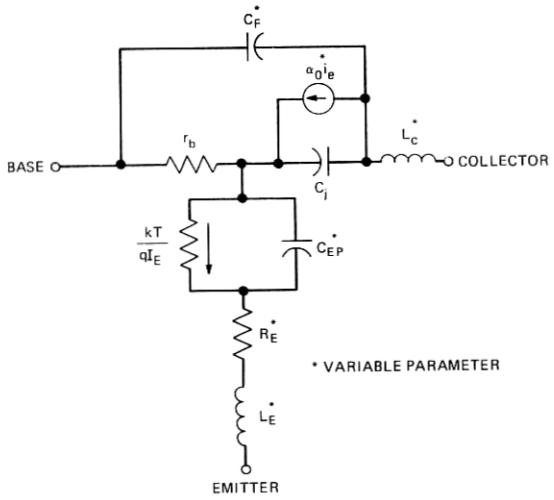

Fig. 10—Circuit model of 82-type transistor.

Table VI — Median transistor parameters

Transistor Type	Function	Bias Volts	Bias mA	Median Parameter Values* α_0	R_E (ohms)	C_F (pF)	C_{EP} (pF)	Stage Placement Criteria
82A	Ampl. stage 1	9.4	50	0.9920	0.173	3.38	128	Noise figure and α_0
82B	Ampl. stage 2	9.2	153	0.9892	0.192	3.29	376	α_0
82C	Ampl. stage 3	9.2	50	0.9885	0.166	3.29	149	C_F
82D	Ampl. stage 4	10.0	147	0.9854	0.189	3.20	419	M_2 and α_0
82E	Ampl. stage 5	10.0	147	0.9881	0.188	3.05	379	M_3 and α_0
82F	Oscillator	8.0	9					$0.9780 < \alpha_0 < 0.9938$
82G	Oscillator	8.0	9					$0.9780 < \alpha_0 < 0.9890$

* Refers to TAT-6 production. The median 30-MHz noise figure for the 82A was 1.87 dB. The median 28.9-MHz M_3 for the 82E was 93.1 dB.

4.6 Surge protection

Two gas-filled electron tubes in each GSF provide the first level of protection against the high-energy surges which accompany faults in the dc power path. These tubes break down at a voltage in the range of 75 to 600 v, depending on the rate of change of the incident surge voltage. Although the gas tubes prevent damage to the passive components, the transistors require a second level of protection which is furnished by reverse-biased diodes (Table VII).

Table VII — Repeater surge protection diodes

Location	No. of Diodes	No. of Diode Packages	Reverse Bias, Volts	Protection Function
Ground separation filter	3	3	12.0	Power path
Preamplifier	2	1	0.86	Amplifier input
Directional filter	2	1	4.0	Amplifier output
Output network	2	2	12.0	Amplifier output

Three Zener diodes in the GSF share equally (within 10 A) peak current surges of up to 160 A caused by the cable discharge, while limiting the voltage across the dc power path to the range −3 to +19 V.

The PWA output transistor proved to be very susceptible to damage from the surge's low-frequency components which pass through the low-band output directional filter. A pair of 4-V reverse-biased diodes placed across the directional filter reduced the surge and also improved the noise-sing stability margin by compressing gain at abnormally high low-band signal power.

Surge protection was probably the most elusive problem encountered in realizing an acceptable repeater design. The results of an extensive testing program in which hundreds of devices were repeatedly surged indicated that the average output stage transistor would survive 50 worst-case surges before failure. Achieving this degree of protection cost what appeared at the time to be a 3- to 4-dB increase in repeater third-order distortion. As further discussed in Section 7.3, the actual degradation was much greater.

4.7 Corona noise

Because of the high voltage present in the repeaters and equalizers, it is possible that static discharges (corona noise) could either excessively degrade system noise performance or lead to an eventual component failure. The requirements adopted were based upon the possibility of insulation damage and failure and are about 20 dB more stringent than current requirements based on group band (48-kHz) data.

Each repeater and equalizer is backfilled with 4.4 atmospheres (50 psig) of dry nitrogen and tested for 21 hours at 7 kV. Broadband detectors, 0.1 to 30 MHz, record all corona "pops" which exceed 1 mV at the output of the repeater. Up to 12 counts exceeding this threshold are allowed in a 21-hour period.

4.8 Passive components

A summary of the types and values of SG repeater passive components[5] is included in Table VIII.

All resistors are the tantalum film type on alumina substrates and have thermo-compression bonded leads.

NPO ceramic capacitors have replaced mica and paper types in all except high-voltage applications. The paper-castor oil high-voltage capacitors are of radically new design, featuring a coaxial structure to reduce parasitic inductance. Tantalum electrolytic capacitors are used for coupling and bypassing purposes where large values are needed.

Ferrite-core chokes, smaller air-core coils for filter networks, and a cavity-tuned inductor are all innovations from previous designs. Hybrid feedback at the amplifier's input and output ports is implemented by means of tightly controlled autotransformers wound on ferrite cores. An autotransformer is also used in the power amplifier to obtain a 2:1 current gain between the Darlington pair driver and the common-base output stage. In the ground-separation filters, coaxial longitudinal chokes help provide the necessary isolation between the amplifier input and output.

4.9 Reliability

As discussed in a companion article,[2] the design objectives for SG component reliability are 0.05, 0.5, and 1.0 FITs (failures in 10^9 device-hours) for passive components, diodes, and transistors, respectively. These levels of reliability have been achieved on previous systems.

Using the preceding reliability objectives and the repeater component count of Table IX results in a repeater failure rate of 21 FITs. (This excludes the oscillator, since its failure would not degrade system performance.)

4.10 Terminations

The cable-repeater terminations, described in detail in a companion article,[3] have a significant effect on system transmission. Although their actual insertion loss is small, about 0.13 dB per repeater at 30 MHz, they contribute a loss ripple due to impedance interactions with the repeater and cable. Reflections occur at each end of the "pigtail," the flexible coaxial transmission lead between the cable and repeaters within the termination. Because the insertion phase of the directional filter and output network varies rapidly with frequency (typically 360 degrees across the high band), the phase of the repeater reflection coefficient across the high band changes by about two revolutions. The reflection coefficient at the cable end of the termination results from excess capacitance in the transition area, 6 pF in the armorless and 3 pF in the armored terminations. The interactions between these two reflections, separated by the electrically long pigtail, causes a rapidly varying loss ripple whose magnitude approaches ±0.035 dB in the high band (see Table IV).

Table VIII — SG repeater passive components

Resistors:

Type	Values (ohms)	Tolerance (percent)	Dissipation (Watts)	Temperature Coefficient (PPM/°C avg)	20-Year Stability (max. percent)
Metal film	3–5000	±0.1 min.	1/16, 1/8	0–40	+0.05

Capacitors:

Type	Values	Tolerance (percent)	Max. VDC	Temperature Coefficient (PPM/°C)	20-Year Stability (max. percent)
Coaxial H-V	0.013 μF	±3	8000	−40	+0.5
Ceramic	5 PF − 0.047 μF	±1 min.	15	±30	+0.02
Tantalum ESR	1–10 μF 2 ohms at 2 MHz	±7	15		

Inductors:

Type	Values (μH)	Tolerance (percent)	Max. DC Current (mA)	Temperature Coefficient (PPM/°C)	20-Year Stability (max. percent)
Air core	0.1–44.3	±1 to ± 10	—	—	—
Torroidal powder core	12.9, 16.25	±3	700	−200	+0.5
Air core slug-adjusted	0.05–5.4	±2 (min. adj)	—	—	—

Transformers:

Type	Remarks
Longitudinal choke	Wound with 50-ohm coaxial cable, 250-μH minimum L to longitudinal currents, max. current 700 mA
Phase reversing	1:1 and 1:−1, 50 ohms, 250 μH min. L, ferrite core
Autotransformers	5:20 ohms and 33.3:50 + 100:150 ohms, ferrite core

Thermistors:

Type	Values (ohms)	Tolerance (percent)	Temperature Coefficient (ohms/ohms/°C)	20-Year Stability (max. percent)
Parallel disks	13.83 at 11.2°C	±1	−0.044 at 25°C	+2
Individual disk	29.0–34.0 at 25°C			

V. EQUALIZER ELECTRICAL DESIGN

For the first SG installation (TAT-6), two types of undersea equalizers were developed, a conventional ocean-block equalizer (OBE) and a special shore-controlled equalizer (SCE). The location in the system of these equalizers and their functions in the overall equalization plan are described in a companion article.[2]

The primary job of an OBE is to equalize the accumulated misalignment at the end of an ocean block. Such misalignment arises from design and manufacturing deviations in both repeaters and cable and from

Table IX — SG repeater component count

Component Type	Ground Separation Filters	Directional Filters	Output Network	Preamplifier	Power Amplifier	Oscillator HB	Oscillator LB	Subtotal
Resistors		4	8	19 or 21	17	9	9	59
Capacitors:								
Ceramic	4	36	19	12	8	6	6	85
Paper	2							2
Tantalum	1	1		6	8		2	16 or 18
Thermistor*				1				1
Inductors:								
Air core		20	11	2	4	3	3	40
Ferrite				4	4	1	1	9
Dust core	2							2
Transformers	2	2		1	2			7
Diodes	2	2		2	1	2	2	9
Transistors				2	3	1	1	6
Gas tubes	4							4
Crystals						1	1	1
Subtotal	17	65	38	51	47	23	25	†

* Thermistor is used only in shallow-water temperature-controlled repeaters. It replaces two resistors.

† Total components: repeater with HB oscillator: 241; repeater with LB oscillator: 243.

uncertainties associated with predicting the overall transmission of the system in the ocean-bottom environment. The OBE is adjusted to its final setting aboard ship shortly before it is overboarded.

The primary job of the SCE is to compensate for transmission changes occurring in one sector over the life of the system. (For TAT-6, a sector is approximately one-fifth of the system length.) From the standpoint of the transmission path, both the OBE and SCE are passive. Gain for equalization is obtained by shortening the cable length between the two repeaters adjacent to an equalizer to a total of one mile (one-half mile on either side of the equalizer). In the lower part of the low band, additional equalization gain is provided by the repeater gain boost.

5.1 Ocean-block equalizer

The SG ocean-block equalizer design retained those features of the SF system OBE that proved so successful in equalizing that system, viz:

(*i*) Independent equalization in the two transmission bands.
(*ii*) Switchable networks—a set of 14 networks (7 per band), identical in all OBEs, that can be individually switched "in" or "out" of the transmission path.
(*iii*) Mop-up networks—a series of up to seven tandem networks in each band that can be designed and fabricated late in the manufacturing cycle of an equalizer. These could be different for each OBE.

The switchable and mop-up equalization modes accomplish the primary OBE function and are discussed in detail in separate sections.

Figure 11 shows the OBE. Since there are no active electronics in the OBE, a power-separation filter (PSF) at each end bypasses the high-voltage direct current. This arrangement places the internal chassis ground at the same potential as the outer pressure housing (sea ground). (The repeater and SCE differ in having the internal chassis at center-conductor potential.)

Separation of the two transmission bands within the OBE is achieved through use of two directional filters, each consisting of a low-pass and high-pass filter paralleled at one end to form a three-port network.

A build-out network in each band centers the switchable network adjustment range around the nominal OBE loss, while preserving the maximum possible flat loss for mop-up network design. Nominal OBE total loss corresponds to that of 4.1 nautical miles of 1.7-in. SG cable at sea bottom plus a loss equal to the per-block repeater gain boost.

A coaxial transmission test lead exits the OBE housing through a high-pressure seal. This lead is used during tests of the assembled shipload of cable and repeaters prior to laying and during measurements between ship and shore while laying.

Within the OBE, the test lead terminates in a symmetrical 3-port splitting pad that can be switched "in" or "out" of the transmission path. After final adjustment on shipboard, the pad is switched "out." This disconnects the test lead and connects transmission straight through. Finally, the end of the external test lead is overmolded.

5.1.1 Switchable networks

The insertion loss functions of the 14 switchable networks are given in Table X. Each network is realized by a constant resistance (50-ohm) structure. Three classes of shapes are identifiable, "root-f," "root-f minus f," and a broad "bump," whose peak loss is near the center of each band. (The latter two shapes have small amounts of root-f loss added to make them physically realizable.) These three shapes are plotted in a companion article.[2] The frequency characteristics of 16 of the total of 128 settings obtainable in the low band are shown in Fig. 12. The switchable networks are capable of equalizing only smooth, relatively broad components of misalignment. (The more ripply components are handled by the mop-up networks.)

Of the three classes of switchable network shapes, the one with by far the largest range is root-f. This is because repeater gain and cable loss, as well as changes in cable loss due to temperature and pressure effects, are approximately proportional to the square root of frequency. It follows, therefore, that residual differences in these parameters, including those due to inaccuracies in predicting sea-bottom temperature or depth

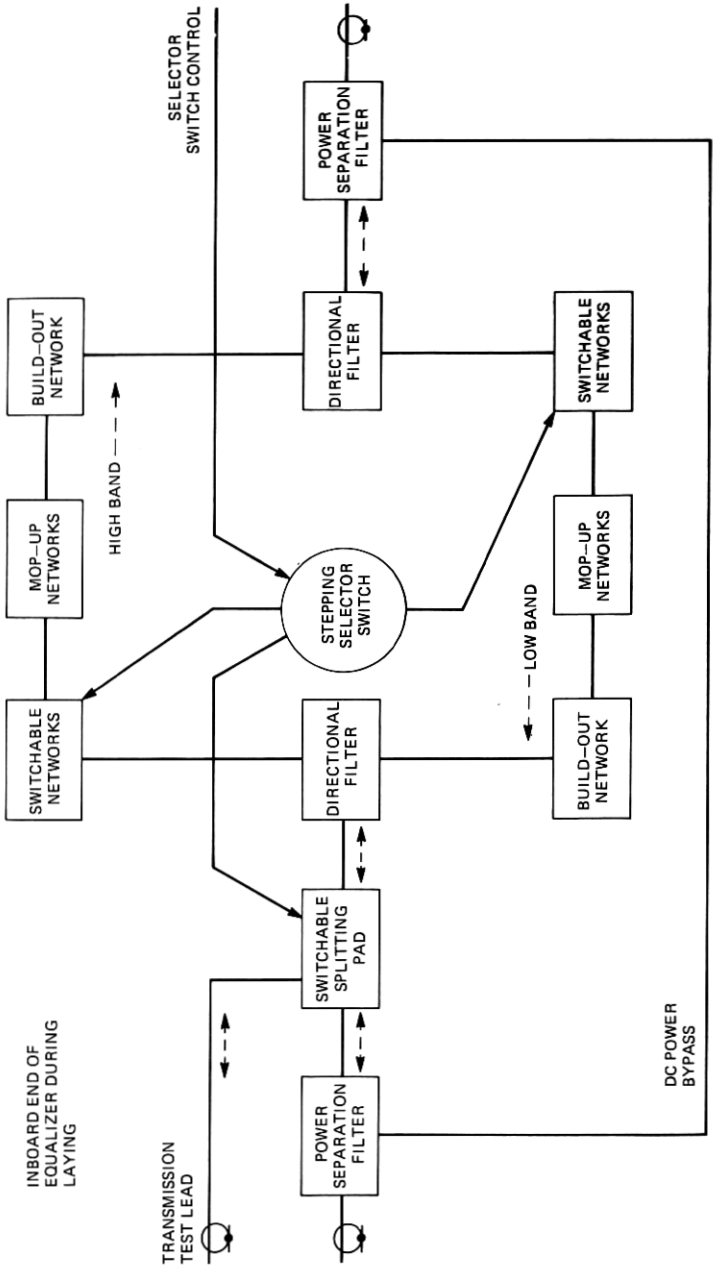

Fig. 11—Block diagram of ocean-block equalizer.

Table X — Ocean-block equalizer switchable loss shapes (dB)

Low Band	High Band
$8\sqrt{f/30}$	$8\sqrt{f/30}$
$4\sqrt{f/30}$	$4\sqrt{f/30}$
$2\sqrt{f/30}$	$2\sqrt{f/30}$
$1\sqrt{f/30}$	$1\sqrt{f/30}$
$8(\sqrt{f/14} - f/14) + 2\sqrt{f/30}$	$17.26(\sqrt{f/30} - f/30) + 0.5\sqrt{f/30}$
$4(\sqrt{f/14} - f/14) + \sqrt{f/30}$	$8.63(\sqrt{f/30} - f/30) + 0.5\sqrt{f/30}$
1.5-dB bump + $\sqrt{f/30}$	1.5-dB dump + $\sqrt{f/30}$

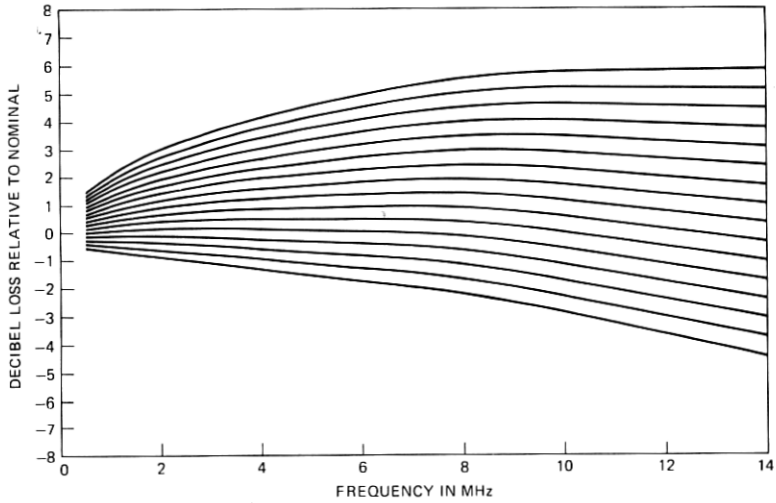

Fig. 12—One-eighth of the possible switchable network settings obtainable in the low band (nominal loss is equivalent to half the total switchable network loss).

produce transmission changes which are roughly proportional to root-f.

The rationale behind giving the "root-f-minus-f" shape the second largest range is more subtle. Consider the following: Cable loss per unit length, α, can be expressed quite precisely as a function of frequency, f, by

$$\alpha = A\sqrt{f} + BDf, \tag{3}$$

where A and B are independent of frequency and D, the dissipation factor, is a measure of the loss due to the cable dielectric. Variations in nominal α for manufactured cable that are due to variations in A are quite closely compensated for over the entire transmission band when each cable section is cut individually to a specified top frequency loss. Variations in B or D, on the other hand, are compensated for correctly only at the cutting frequency, because one is attempting to correct an

attenuation error that is directly proportional to f* by varying a loss that is closely proportional to $\sqrt{f}$. (For SG cable, at 30 MHz the first term in eq. (3) is 94 percent or more of the total.) The resulting misalignment is compensated for reasonably well in the OBE by the root-f-minus-f switchable shape.

The third switchable shape, the broad bump, is the only one that is not specifically cause-associated. However, the root-f shape has its greatest effect toward the top of each band, and the root-f-minus-f shape has its greatest effect near the bottom. Thus, the bump, whose effect is primarily in the middle of each band, provides a general-purpose equalization characteristic to the switchable networks.

Associated with each switchable network (and the test-lead splitting pad) is a small magnetic latching double-transfer relay. These relays are set to one of two possible states by means of a stepping selector switch. The stepping selector is operated by a series of pulses of either polarity applied to the switch control lead that enters the OBE housing at the end opposite the transmission test lead (Fig. 11). The selector is a single-pole, 16-position switch, each position associated with a particular relay and network, or with a reference condition. Each pulse applied to the switch control lead accomplishes two functions. First, it advances the selector one position (independent of pulse polarity). Second, a positive pulse switches the network (relay) associated with the new position "out," whereas a negative pulse switches the network into the transmission path.

5.1.2 Mop-up networks

In contrast to the switchable mode, two features of the mop-up networks worth noting are:

(*i*) Their ability to provide fine-grain (i.e., ripply) compensation.
(*ii*) The relatively short interval required between design of these networks and completion of manufacture of the OBE.

To achieve these features, each mop-up network uses a modular-design, constant-resistance (50-ohm) bridged-T configuration constructed from a predetermined stockpile of components and standardized hardware.† Parasitic circuit effects of components and hardware have been well-characterized in advance, because there is no time for the usual engineering development to assess and correct second-order effects. Specially written computer programs are used to expedite design and documentation effort. Network performance is computed taking into account the effects of parasites and discrete component values, and elec-

* This is not strictly true for variations in D which can be frequency-dependent, but the point is still valid.

† This ensures that aged undersea cable quality components are available simultaneously with a network design.

trical test specifications are generated for both individual networks and tandem assemblies. The OBE is designed so that the complete equalizer, less mop-up networks and high-pressure housing, can be constructed and tested before mop-up design information is available.

An individual bridged-T network can provide a positive bump shape (loss vs frequency), a negative bump (dip), simple low- or high-pass shapes, or flat-loss. Networks can be connected in tandem (with minimum interaction due to the constant resistance design) to obtain combinations of these shapes. In practice, most mop-up networks are the bumps or dips, whose circuit configuration is shown in Fig. 13. For a fixed characteristic impedance, R_0, such simple shapes can be completely specified by peak (bump or dip) amplitude, center frequency, and stiffness (which can be defined as the ratio of upper half-loss frequency to center frequency).

The range chosen for the SG mop-up component stockpile is shown graphically in Fig. 14. The symmetry of this figure results from the nature of the bridged-T for bump and dip shapes which calls for a pair of LC resonance values that intersect equidistant from the horizontal R_0 line along a vertical line corresponding to the center frequency. Similarly, the pair of shunt and series resistance values falls equidistant above and below the R_0 line in Fig. 14. In some cases, when a network design calls for component values outside this range, a flat-loss network transformation can be applied which moves the required values inside the stockpile range. The resulting transformed network then has a loss which is the sum of the desired loss shape and additional flat loss.

The designer of mop-up networks must "spend" his flat loss wisely, because the available flat-loss is limited to 9.5 dB in the low band and 12.5 dB in the high band. The number of mop-up networks in a particular OBE could be less than the seven per band allowable from physical

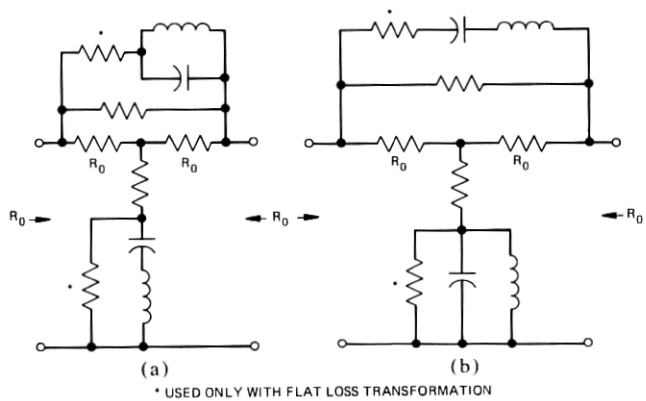

Fig. 13—Mop-up network configurations. (a) Loss dip. (b) Loss bump.

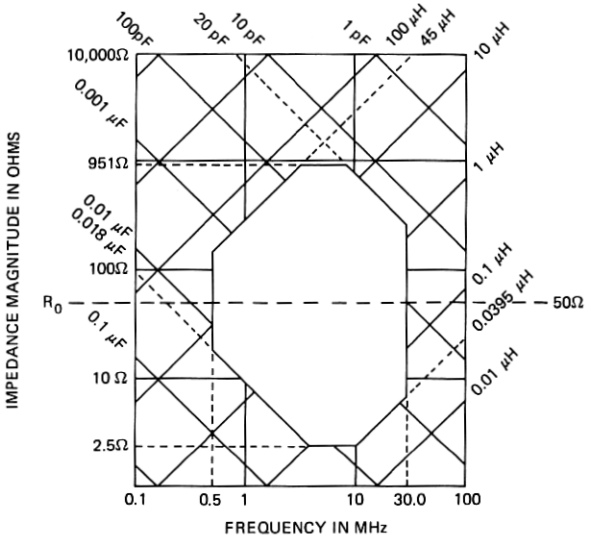

Fig. 14—Stockpile range.

Table XI — Passive OBE components

Component	Description	Value	Tolerance (percent)	Use
Resistor	Wirewound, vitreous enamel, power resistor	14.0 ohms	±1	Selector switch circuit
Capacitor	HV oil-impregnated, paper dielectric, housed in ceramic cylinder with metal end caps	0.02 μF	±3	PSF(A) and (B) assemblies
Inductor	Duolateral-wound over plastic form capable of continuous operation with up to 0.7 amperes through windings	1.0 mH	±5	PSF(A) and (B) assemblies
Selector-switch	18-point, unidirectional switch			
Relay	"Crystal can" size, hermetically sealed, magnetic-latching relay containing two transfer break-before-make contacts with No. 1 contact metal. Relay has an H-shaped spring-supported armature-magnet assembly and an isolated, hermetically sealed coil chamber.			

constraints because of the limited amount of flat loss which is available.

5.1.3 Components

With the few exceptions noted in Table XI, all components used in the ocean-block equalizer are identical in type with those used in the repeater, which have already been described.

5.2 Shore-controlled equalizer

Because of uncertainty in the long-term stability of cable loss, plans for the earlier SD and SF systems had included shore-controlled equalizers (SCEs). In both cases, however, development effort on the SCEs ceased when adequate cable loss stability was assured. Based on this experience, the SG system development began assuming SCEs would not be required. In mid-1975, six months prior to the beginning of the first deep sea lay of TAT-6, cable loss changes noted in factory measurements[3] clearly indicated the necessity for installing SCEs. Development was started in August 1975, less than six months before the date the first unit was due to be shipped. This extremely short time interval required the use of readily available components.

5.2.1 SCE realization

The SCE has much in common with the OBE: directional filters, switched network configuration, and certain hardware. The OBE stepping-selector switch is replaced by an instrument-type 50-mW dc motor and gear train furnished by CIT.* A modified repeater GSF replaced the PSF of the OBE, and a final gear reducer and wafer switch assembly were procured from commercial sources. Special filters, amplifiers, and rectifiers using available and aged SG components were designed to control the electromechanical switching operation.

5.2.2 Method of control

The SCE uses the same type of magnetic latching relays as the OBE for switching networks in or out of the transmission paths. Relay states in each SCE are controlled by two unique frequencies spaced 400 Hz apart in the 11.464- to 11.472-MHz band. As shown in Fig. 15, the two signals transmitted from the A terminal are selectively amplified and rectified in the SCE to produce two dc control voltages. The output of the motor channel powers the motor which turns the selector switch; the output of the relay channel, when present, serves as an "activate" signal for the latching relays as they are sequentially accessed by the selector switch. Position identification information is transmitted back to the A terminal by amplitude modulating the second harmonic of the motor channel frequency. Two adjoining selector positions are associated with each relay and network. One position corresponds to switching the network in, and the second corresponds to removing the network.

* Compagnie Industrielle des Télécommunications.

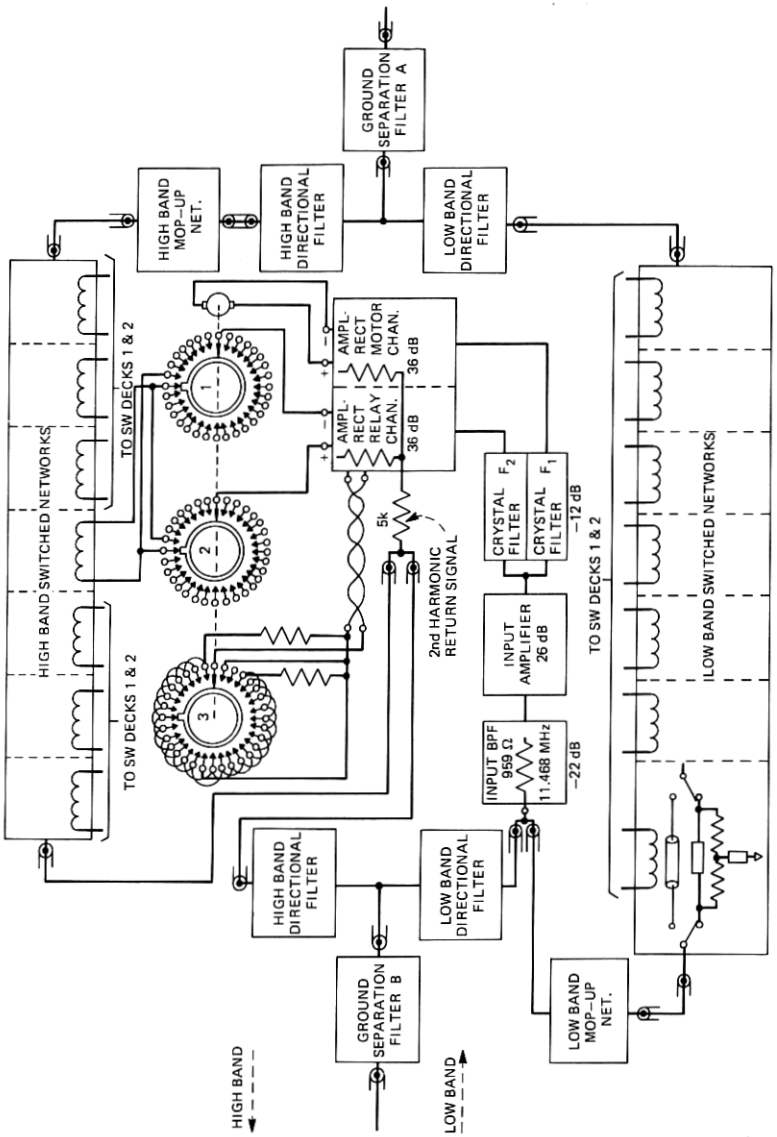

Fig. 15—Block diagram of SG shore-controlled equalizer.

Figure 16 is a chart recording of the second harmonic signal as received during an SCE-adjusting operation. The annotations indicate the loss shapes of the seven switchable networks in each band. Individual networks are switched in or out by transmitting a short burst (2–3 s) of the relay channel tone during the interval, typically 12 s, that the network coil is connected to the relay channel rectifier. By monitoring the level change of a supervisory tone which goes through the SCE, one can verify immediately that the network has switched.

Figure 17 shows the typical characteristics of the two control channels. The SCE is normally left in the index position after adjustment. In this position, the relay channel rectifier is connected to a diode rather than a relay coil. As the relay channel signal level is slowly increased, the second harmonic return increases smoothly until an abrupt step of about 20 dB occurs, indicating that the rectifiers have begun to conduct. This point serves as a reference level; a signal 12 dB above the reference will produce sufficient power to switch a relay. The motor channel characteristics are similar. The control tones are tuned to the precise center frequencies of their respective crystal filters by monitoring the returned second harmonic signal.

5.2.3 Control system design

The control system of the SCE is a modified version of that used in the French S-25 system designed by Compagnie Industrielle des Télécommunications. The success of the accelerated SCE project is largely due to the cooperation of CIT in sharing their knowledge and experience and in furnishing the critical motor-gear train assemblies.

A number of measures prevent false operation of the SCE. The control frequency band, 11.464 to 11.472 MHz, is a space between supergroups normally used for noise monitoring. A band elimination filter at the A terminal blocks undesired incoming signals in this band. The operating level for the control tones was chosen sufficiently high, up to −6 dBm at repeater output, to preclude the possibility of inadvertent operation. The second harmonic return signal exceeds the system background distortion by at least 20 dB. From the normal "rest" position of the controls, *both* F_1 and F_2 must be applied to change the SCE setting.

5.2.3.1 Filters. The input bandpass filter, centered at 11.468 MHz, is an LC type with a 4-dB bandwidth of 0.5 MHz and is designed to operate between 1000- and 50-ohm impedances. Together with the 959-ohm isolation resistor, it has a through loss of 22 dB and adds less than 0.2-dB bridging loss to the low-band transmission path.

Each crystal filter contains a single crystal of the same design used in supervisory oscillators. The crystal, with a series resistance of 20 to 36 ohms, operates in series between impedances of typically 5 ohms. Each filter provides at least 34 dB of adjacent channel suppression (400 Hz away) while adding 12 dB of flat loss.

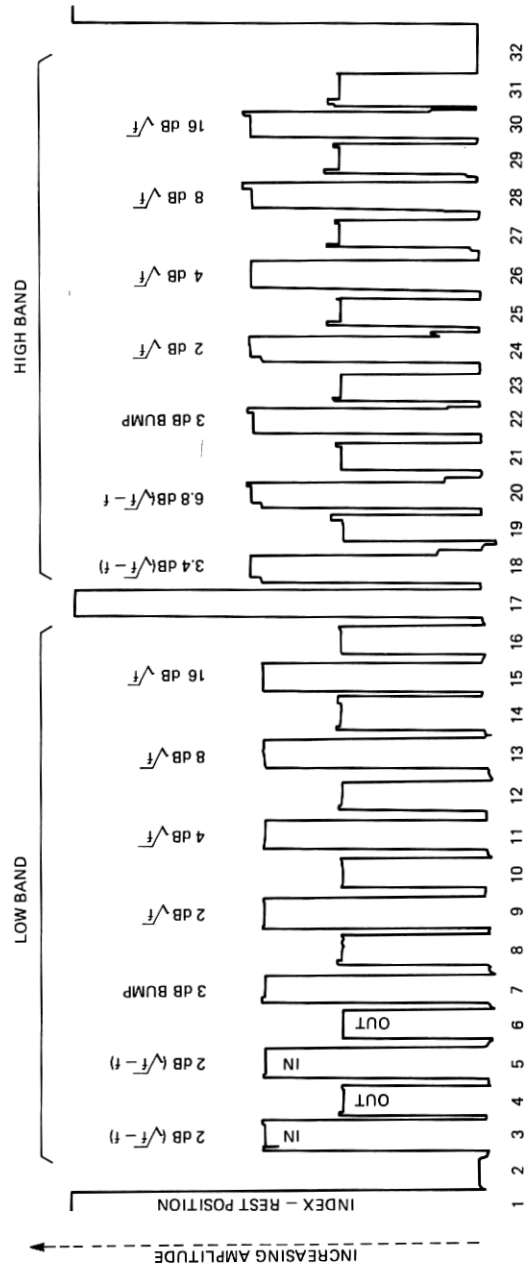

Fig. 16—Shore-controlled equalizer—second harmonic signal, $2F_1$, returned to shore during adjustment.

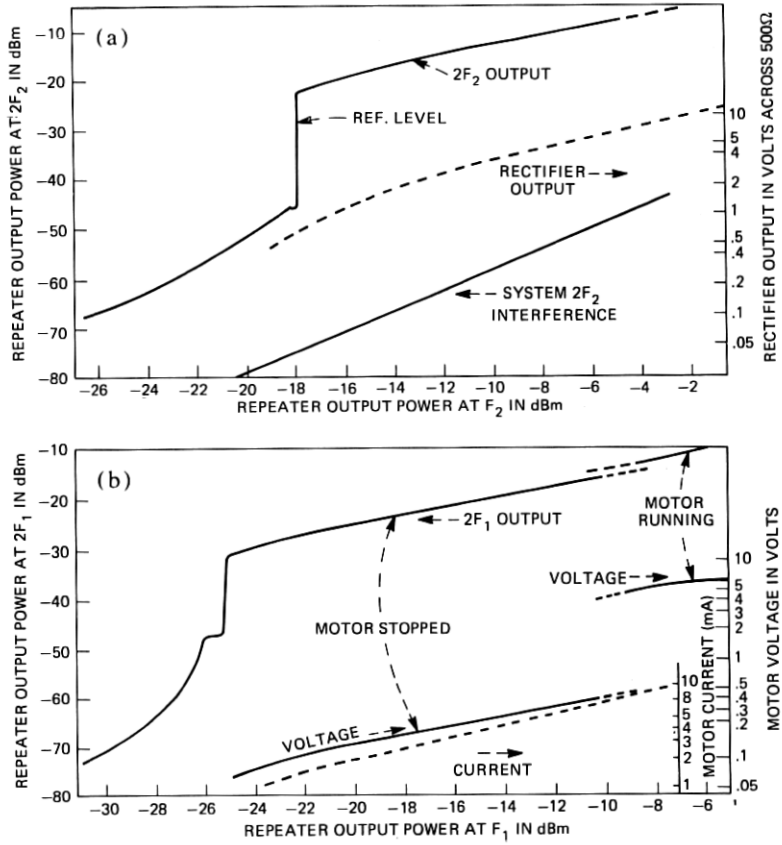

Fig. 17—(a) SCE relay-activate channel characteristics. (b) SCE motor channel characteristics.

5.2.3.2 Amplifiers. The three amplifiers are identical except for gain and terminations. Each has two common emitter stages with gain controlled by feedback and each is biased at 12 V, 219 mA. The input amplifier has 26-dB gain and 50-ohm input and output impedances. Each power amplifier provides a nominal gain of 36 dB. The power amplifier input impedances are low, as required by the crystal filters, and the outputs are tuned to operate efficiently into a voltage doubler-type rectifier. The actual gain of each power amplifier is tailored, by choice of feedback resistor, to accommodate the loss of its associated crystal filter. The gains and losses are arranged so that each rectifier will deliver 50 mW (5.0 V, 10 mA) to its load (motor or relay) when the signal power at the SCE input is −8 dBm. Each amplifier rectifier will deliver a maximum output power of at least 200 mW.

5.2.3.3 Electromechanical. A precision-instrument-type, permanent magnet, dc motor drives an attached 2000:1 ratio gear train. A 15:1 worm

gear which connects to the wafer switch assembly provides the final reduction. Each of three identical switch wafers has a single pole and 32 positions, 31 of which are active. Two of the wafers connect to the relay coils. Each coil requires two positions, one for switching the network in and one for switching the network out. The third wafer is used as a four-level loss switcher which amplitude-modulates the power of the second harmonic return signal as the switch slowly turns. This return signal informs station personnel of the select switch position.

5.2.4 Future improvements

Since completion of TAT-6, a solid-state circuit has been developed to replace the motor-switch assembly. The remaining components in the SCE are virtually unchanged.

5.2.5 Switchable range

The switchable loss shapes available in the SCE are listed in Table XII. The networks are similar to those in the OBE except that the range and step sizes are twice as large. The SCE has no mop-up network capability.

VI. MANUFACTURING

6.1 Schedules and production rate

Repeater and equalizer final assembly and much of their manufacturing were done at a special factory in Clark, N.J. as with earlier repeaters for SD and SF.

Authorization to proceed with production was received in February 1972, with the first repeater scheduled for shipment in December 1974. Prior to the start of manufacturing, it was necessary to design new manufacturing and test facilities required to handle the SG hardware and the increased frequency range.

Because of the mid-1976 service date of TAT-6 and because the system called for over 800 repeaters and equalizers, it was necessary to achieve

Table XII — Shore-controlled equalizer switchable loss shapes (dB)

Low Band	High Band
$16\sqrt{f/30}$	$16\sqrt{f/30}$
$8\sqrt{f/30}$	$8\sqrt{f/30}$
$4\sqrt{f/30}$	$4\sqrt{f/30}$
$2\sqrt{f/30}$	$2\sqrt{f/30}$
$8(\sqrt{f/14} - f/14) + 2\sqrt{f/30}$	$34.52(\sqrt{f/30} - f/30) + 2\sqrt{f/30}$
$8(\sqrt{f/14} - f/14) + 2\sqrt{f/30}$	$17.26(\sqrt{f/30} - f/30) + 0.5\sqrt{f/30}$
3-dB bump + $\sqrt{f/30}$	3-dB bump + $\sqrt{f/30}$

production capacity of 16 units per week. Concurrently, it was necessary to maintain capacity for other systems at a rate of three units per week.

6.2 Environmental conditions

All critical assembly operations are performed in "clean" rooms where temperature, humidity, and airborne contaminants are closely monitored. Objectives are less than 50,000 dust particles above 0.5 microns per cubic foot, temperatures of 22.8° ± 1.1°C (75° ± 2°F), and relative humidity of less than 40 percent. In the paper capacitor winding room, relative humidity is controlled to less than 20 percent. Dust counts on three sizes of particles (0.5, 1.0, and 2.0 microns) are monitored weekly for each clean room. Positive air pressures are maintained and monitored in all rooms and associated vestibules to prevent entry of contaminants.

6.3 Product development and manufacturing facilities

The design of the SG system required improved manufacturing and test facilities. The purpose of these facilities was to enable the manufacture, aging, and testing of new components such as ceramic capacitors, to provide new transmission test facilities, and to provide new and improved facilities for closure type operations. Development work on facilities began at Clark, N.J. in February 1971.

6.3.1 Aluminum castings

The large number of repeaters and the elimination of the hermeticity requirement for the electronics unit required that more economical procedures for making aluminum castings be investigated.[7] The investigation revealed that the castings should be made from the low-pressure permanent mold (LPPM) process and the cylinder should be extruded. Expensive machining operations were virtually eliminated with no sacrifices in quality. In addition, the separate, one-piece cylinder simplified the epoxy coating procedure and subsequent assembly with the main frame, which simply slides into the surrounding cylinder, where it is locked in place.

6.3.2 Ceramic capacitors

Ceramic capacitors, new to undersea cable application, were substantially different from their predecessor,[8] the mica capacitors, both in physical appearance and electrical characteristics (Fig. 18). Their use in SG circuits was mandated by the need for smaller encapsulated units having negligible parasitic inductance. Replacement of mica with ceramic also reduced costs and avoided a serious procurement problem, that of purchasing top quality mica.

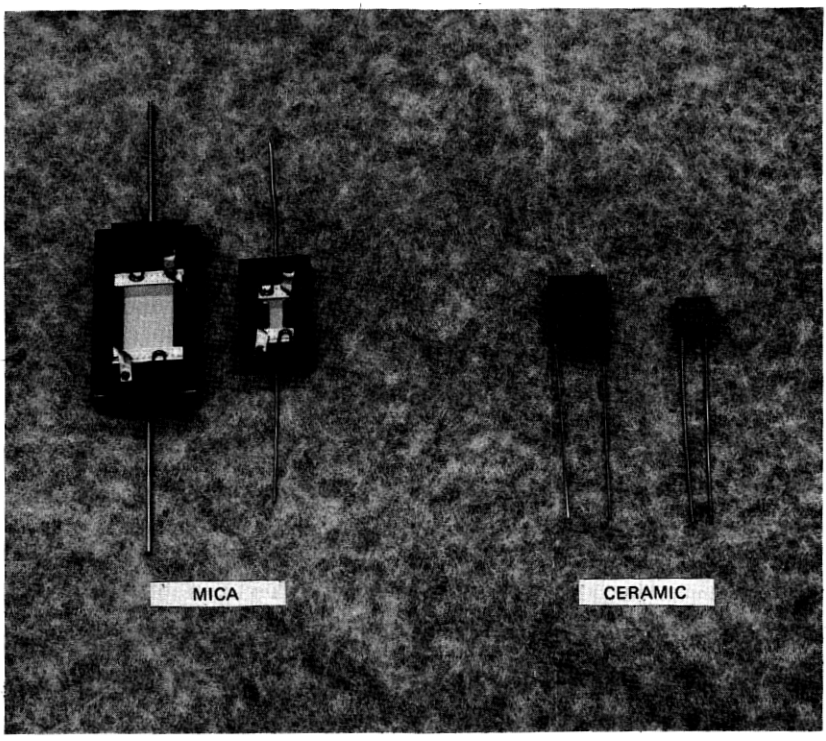

Fig. 18—Comparison of ceramic and mica capacitors.

Although ceramic capacitors are purchased from commercial suppliers, prior to manufacture of electronics, complete in-house qualification procedures had to be specified and implemented. Principal tests performed included insulation resistance, dielectric strength, capacitance, and conductance along with 17 weeks of voltage conditioning aging (see Fig. 19).

Because of its physical design, the ceramic capacitor was readily adaptable to automatic testing methods. Special test processing fixtures were provided onto which 25 capacitors were attached for processing through the full complement of tests. Flexibility was designed into the fixtures, enabling the capacitors to be tested individually for capacitance, conductance, and insulation resistance, or as a group of 25 as is required during aging and breakdown testing. Because of stringent tolerance requirements, 0.1 percent in some cases, test set accuracies and repeatability has to be in the order of 0.01 percent. Special design features such as gold-plated contact points on fixtures and shielding to eliminate stray parasitics were necessary.

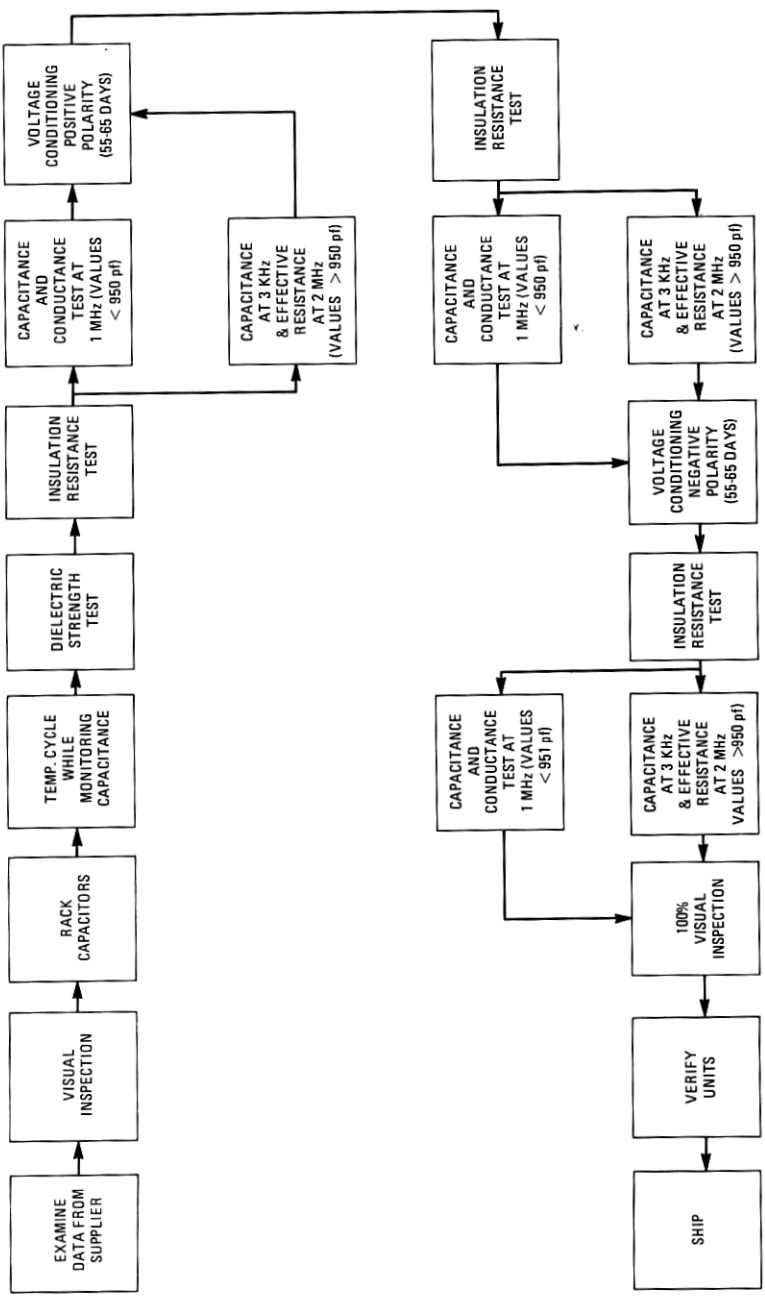

Fig. 19—Ceramic capacitor process flow chart.

6.3.3 Printed-wiring-board assemblies

From a manufacturing viewpoint, one of the significant changes in physical design was the use of printed-wiring boards (PWB). PWB requirements and assembly techniques were developed with specific attention to component mounting procedures, fixturing, and soldering techniques. Overlays were provided to assist the technician in proper location of components. In addition, training programs were developed to acquaint the operators and inspectors with component identification, and to identify various component and board defects which could degrade reliability.

Detailed investigations were undertaken to establish improved board manufacturing processes and requirements. Plating procedures were revised and improved at printed-wiring board manufacturing locations. New visual standards to aid in judging dewetting of solder-coated circuit paths were also developed.

6.3.4 Seals

The function of the high-pressure seal is to provide a dc power and signal transmission path into the high-pressure housing. It must withstand high dc voltage and full sea pressure, while maintaining a satisfactory coaxial transmission path. The seal chosen for the SG repeater and equalizer was a modified version of the 8-type seal manufactured at Western Electric's Burlington, N.C. plant. Its predecessor, the 3-type seal used in SF, did not have suitable transmission properties in the SG high band.

The primary sealing mechanism in both seals is the thin polyethylene gasket adjacent to the ceramic. In the 3-type, the ceramic is backed up by a large metal disk which provides satisfactory mechanical performance but introduces excessive capacitance with respect to the 50-ohm transmission impedance. The metal disk was eliminated in the design of the 8-type seal and a larger ceramic cylinder was used. This produced a suitable mechanical seal and at the same time reduced the capacitance to provide proper transmission impedance.

The 8-type seal (Fig. 20) was completely molded in one operation, including attachment of both pigtail leads, rather than three molding operations needed for the 3-type seal. This resulted in reduced cost and increased production capacity from each molding press.

The most severe problems encountered in developing the 8-type seal involved the feed-through assembly. The copper caps on the ends of the ceramic are provided to control electric field strengths. Initially, these were brazed to the ceramic to provide hermeticity in the assembly, but forces generated in the molding operation were sufficient to break the ceramic adjacent to the braze joint, destroying the hermeticity. This problem was overcome by making the conductor in two parts with the

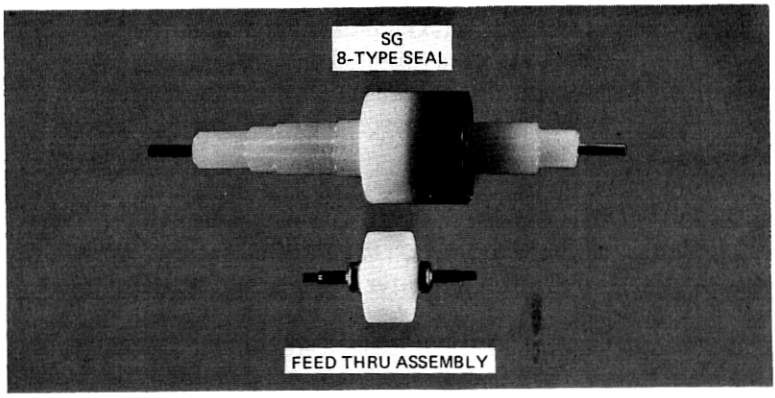

Fig. 20—High-pressure seal.

cap configuration integrally formed on each. These are assembled to the ceramic part (with small fluoroplastic washers between the ceramic and the caps) and screwed together with a coupling sleeve within the hole in the ceramic. A small slug of solder is included in this assembly. The unit is then heated to melt the solder into the threads and the threads are torqued hand tight. Upon cooling, the conductor parts are fused together. Differential thermal shrinkage compresses the fluoroplastic to form a hermetically sealed assembly.

This design change eliminated the need for metallizing the ceramic and brazing the caps to the ceramic, reduced the cost of the feed-through assembly, and produced a higher quality seal.

6.3.5 Subassembly and final repeater testing

Early in the planning, it was decided that the bulk of the transmission testing would be performed by a computer-operated transmission measuring set[9] (COTMS). Duplicate sets were provided. Choice of the COTMS was based on: (*i*) its ability to handle a measuring sequence automatically, including recording and interpreting results, and (*ii*) its precision, repeatability, and precision up to the prescribed top frequency. The COTMS has an accuracy with measurement-averaging of within 0.001 dB. Full utilization of the COTMS included time-sharing of the main measurement unit via remote stations, and formulation of programs specifically tailored to the product needs.

Software packages provided specific instructions to the tester so that type of unit, operation to be performed, and serial number could be double-checked prior to the start of testing. In addition, the software packages identified the proper sequence of test frequencies, checked test results at each frequency against specified limits, and stored a test history for each unit. CRT display units were used as input and output devices

to provide communications between the tester and the computer-monitored test facility. Data were collected on disk and later transferred to magnetic tape for analysis and storage. With the above programming and proper use of remote stations, a test capacity in excess of 20 repeaters per week was attained.

In addition to the COTMS facilities, a precision-adjusting test facility known as MINI-COTMS was also needed. Although called a MINI-COTMS, it bears little resemblance to the COTMS described above. Application of this facility was confined to repeater network and equalizer network tuning.

In the repeater network, five inductors are available for final tuning. Nominal gain for each of 118 discrete in-band test frequencies is stored in computer memory, while deviations from nominal for each frequency are visually displayed on the MINI-COTMS. A special program and adjusting procedure had been formalized which enabled the tester to minimize deviations at most in-band frequencies. The true value of this facility is readily apparent during adjustment, since some of the inductor adjustments interact with one or more others. In this situation, it is a great advantage to have the entire range of frequencies displayed on the CRT output. (Insertion loss measurements are displayed with a precision of ±0.015 dB.) The CRT output, which includes the RSS value of the gain deviation, is observed by the tester while he is performing the final tuning operation. Maximum deviations allowable are of the order of ±0.05 dB with the number of peaks being minimized. Hard copy output is obtained in two forms: values printed to the thousandth of a decibel and a plotted form. Optimum adjustment and use of results to apply corrective action led to minimum deviations among repeaters, which in turn led to a more readily equalizable system and more voice channels.

Equalizer adjustment procedures are similar to the procedures used to tune repeater networks but on a larger scale, with two parameters (insertion loss and return loss) being monitored. Over 70 inductors per equalizer are adjusted on this facility, with a maximum of 14 appearing on any one subassembly. Without a facility having the interactive capability and accuracy of MINI-COTMS, equalizer adjustment would have been virtually impossible.

Other facilities designed for network testing were the crystal oscillator test set, accurate to within 0.1 Hz in the 27-MHz frequency range, a noise and modulation test set, and coarse adjustment (±0.1 dB) test facilities.

6.3.6 Corona testing

Repeaters have been designed to eliminate corona. However, disturbing "pops," or electrical discharges, can be generated under certain conditions. "Pops" above certain voltage levels can cause errors in data

transmission, degrade the quality of voice transmission, and deteriorate insulation.

For SG, extensive effort was spent on developing corona detection equipment and trouble-shooting techniques. A new wide-band detector was designed with the capability of detecting all possible wave shapes with uniform sensitivity across the 30-MHz transmission band. A 2.44-m × 3.66-m shielded room was constructed to provide for high production levels and stringent shielding requirements and to house the product during test. The capability of testing ground separation filters in a pressurized state was also provided. Experience obtained on previous projects proved that pressurizing tends to retard corona impulses. This is an acceptable procedure since final repeaters are pressurized with 4.4 atm (50 psig) of dry nitrogen. In actual production, 12 fixtures were provided and used with a majority of the ground separation filter testing performed with 1.68 atm (10 psig) of dry nitrogen applied to the product.

6.3.7 Closure

Operations associated with closure of the repeater required some completely new facilities as well as an upgrading of existing facilities. Among the more significant changes were: introducing eB (electron beam) welding for joining the high pressure end covers to the copper beryllium housing, instituting a low-pressure test for checking the prime sealing surface of the seal, and modifying vacuum-drying facilities to enable this operation to be performed in the assembled repeater stage of production.

Seals were tested at low pressure to check the mating of the prime sealing surface of the high-pressure seal to the surface of the high-pressure end cover. In performing this test, an O ring and seal are assembled into a high-pressure cover under a small axial load. This relatively minor load, compared to the load when subjected to ocean-bottom pressures, permits the prime sealing surfaces to be tested without fear of the seal bulging to form a side or secondary seal. Helium at 7.8 atm (100 psig) is applied to the seal for two hours. The leak rate of helium past the O ring and prime sealing surfaces, plus migration through the polyethylene body of the seal or along the interface of the internal feed-through, is monitored with a mass spectrometer.

Because of the elimination of a sealed inner unit, the vacuum-drying operation had to be performed in the final stage of manufacture (unit sealed in its copper beryllium housing). This meant that existing facilities had be to modified to:

(*i*) Include heating blankets that reduced the heat losses and were capable of heating the large copper beryllium housing to a temperature of 57°C (135°F).

(*ii*) Handle a 500-pound (227 kg) repeater.

6.4 Quality and verification of product

Manufacture of submarine cable repeaters and equalizers places emphasis on ensuring long-term stability and system reliability. To achieve this end, factors such as training personnel, maintenance of a clean work environment, and adherence to detailed processing specifications were stressed. A series of multiple inspections includes audits of procedures, methods, drawings, and product to assure conformance. These are all vitally important. For TAT-6, over 12,000 items of component performance data were transmitted on a daily basis to the data center for analysis, subsequent statistical manipulation, and finally storage.

As previously mentioned, transmission tests on the electronic subassemblies were performed and verified by the COTMS test facility. These measurements were immediately compared against specified limits, thereby providing instant feedback as to the acceptability of the unit tested. This instant feedback feature was important since it enabled engineering to investigate the cause of unusual test results while a unit was still in the original "fixtured" condition. Data were analyzed for trends so that impending out-of-limit conditions could be detected and compensating adjustments made before serious problems developed. Statistical data were also used as a basis for analyzing out-of-limit conditions and determining proper resolution.

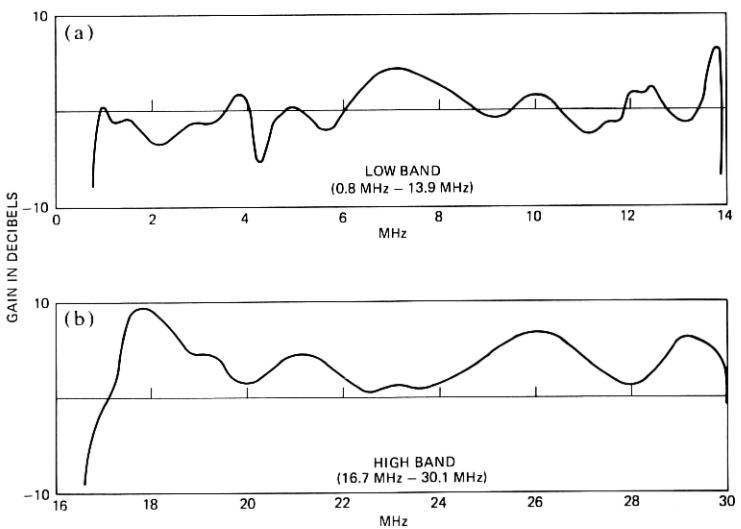

Fig. 21—TAT-6 undersea system misalignment.

Although the aging and testing program is time-consuming, it provides maximum assurance that system components will operate for their intended life.

Equally important with aging and test programs are the procedures which ensure that physical design requirements have been met and that accurate data have been transmitted. It is also necessary to insure that all operations, inspections, and deviations have been properly recorded. For these purposes, multiple inspection procedures are used. First, all operations, inspections, and tests are documented and verified by the signature of the person performing the operation. Second, product examiners verify that prior operations have been performed satisfactorily through entries on data sheets. Third, before any apparatus item (component or subassembly) can be shipped, inspection must verify that all operations have been properly performed.

All data pertinent to the assembly and test of a repeater likewise are compiled in a data book prepared for that specific repeater. This data book is verified for completeness and conformance by a Western Electric Auditor of Manufacturing Practices (AMP). The pertinent data (primarily electrical) are also checked by a resident Bell Laboratories engineer.

As an additional check of quality, the AMPS perform an independent random check of product previously accepted by product examiners.

The Quality Assurance Organization, independent of Western Electric product engineering, is responsible for preparing and performing quality surveys in collaboration with their Bell Laboratories counterparts. One such Bell Laboratories QA engineer is resident at Clark. QA surveys cover detailed investigations of compliance with specified procedures, methods, and drawings in all manufacturing areas.

VII. TAT-6 EXPERIENCE

7.1 Undersea system misalignment

The net misalignment of the TAT-6 undersea system is shown in Fig. 21. The low and high bands contain 53 and 54 supergroups, respectively, including the frequency bands occupied by the order wire and supervisory tones. As indicated in a companion article,[2] the repeater level variation at some frequencies exceeds the end-to-end misalignment. The unpredicted repeater gain deviations arose largely from reflections between the repeater and the cable terminations. The design of the OBE mop-up networks was based upon transmission information obtained from measurements and computer simulation of prototype cable terminations. Evidently, the measured samples of terminations were not representative. With the completion of the first deep sea lay, it was obvious that a special OBE mop-up design would be required following each lay to maintain the misalignment within acceptable limits. Manufacture

of the first such special OBE was completed within a period of two weeks following availability of new mop-up network designs. The OBE was installed near the beginning of the second lay.

7.2 Noise performance

The measured thermal and second-order noise performance of TAT-6 was both satisfactory and consistent with predictions. Third-order intermodulation noise in the top part of the high band, however, exceeded our predictions by as much as 18 dB. The signal-to-noise ratios obtained by noise loading tests during commissioning are shown in Fig. 22. To minimize the total noise at high frequencies, repeater levels were lowered roughly 6 dB. Both the measured and the predicted 29.182-MHz signal-to-noise ratios are indicated in Fig. 23. Third-order intermodulation distortion normally increases 3 dB per 1-dB increase in signal level. On TAT-6, we observed a ratio that varied between 3:1 at low signal levels to 1.8:1 at high signal levels. Narrow-band noise loading tests (2 to 10 supergroups) indicated that most of the third-order distortion was generated by signals close to the frequency of the measured channel.

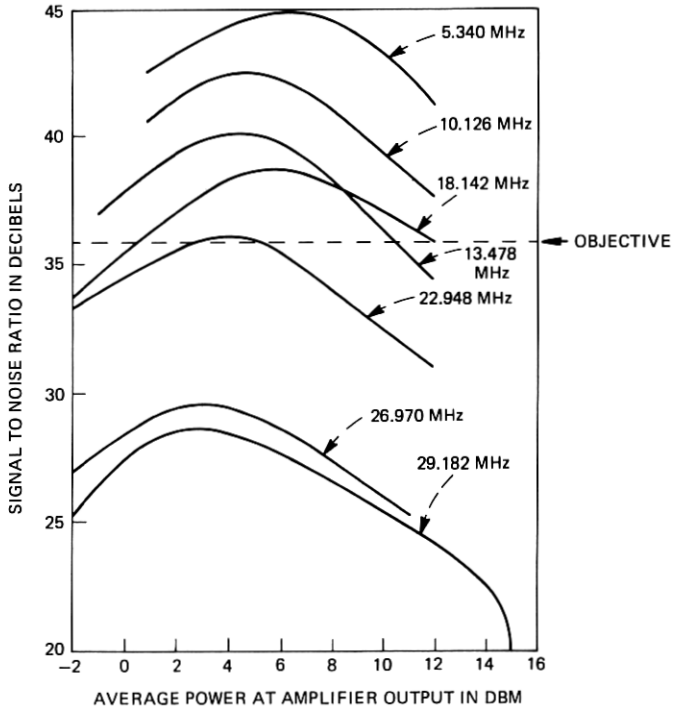

Fig. 22—TAT-6 measured signal-to-noise ratio.

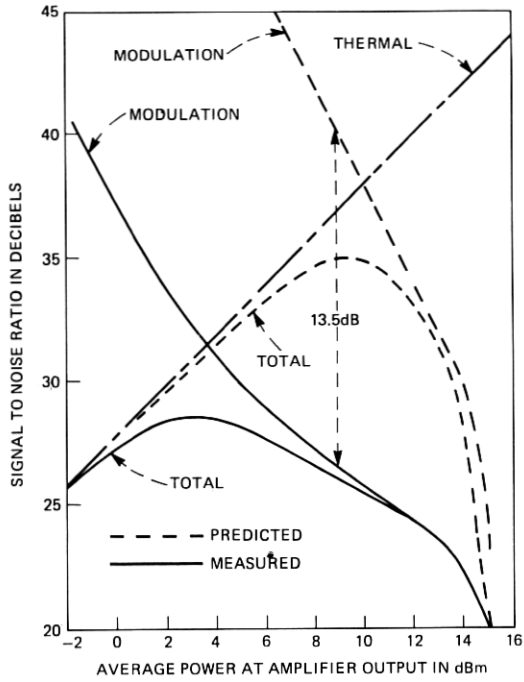

Fig. 23—TAT-6 measured and predicted 29.182-MHz signal-to-noise ratio.

7.2.1 Characterization of M_{3E}

Calculations of system intermodulation noise were based upon average repeater levels, repeater delay characteristics, and repeater modulation coefficients, each being a function of frequency. The modulation coefficients M_{2E} and M_{3E} were characterized in the same manner that had been successfully used in past systems.

A repeater is loaded with three or more fixed fundamental tones of frequencies A, B, and C. Various product frequencies of the type $A \pm B$ and $A \pm B \pm C$ are measured. In the simplest case when the amplifier output stage is the dominant source of distortion, the coefficients M_{2E} and M_{3E} depend only on the product frequency and not on the specific fundamental frequencies. If there is significant dependence on fundamental frequencies, one must consider the effects of signal shaping and delay distortion in choosing the single most appropriate value of a particular modulation coefficient for use in calculating system noise.

In developing the SG repeater, the following fundamental frequencies were used to evaluate repeater intermodulation: 5.8, 14.5, 15.2, 16.6, 21.7, and 27.5 MHz. Nine different third-order and 17 different second-order product frequencies were measured in characterizing the repeater distortion coefficients. In addition, the distortion was measured at two different power levels, +5 and +12 dBm per tone.

Discovery of the excessive third-order intermodulation noise on TAT-6 triggered an intensive search for the source. Instead of measuring repeater distortion with fixed fundamental frequencies, fixed pairs of bandstop-bandpass product-frequency filters and continuously variable fundamental frequencies were used. A contour plot of the measured 3-tone ($A + B - C$) distortion at 26.6 MHz and 2.5°C is shown in Fig. 24 with A and B as the independent variables. (Frequency C depends on A, B, and the product frequency.) Frequency triplets that produce equal distortion are connected with "isomodulation contours." The distortion increases with the frequency of each fundamental and the product. Also the distortion tends to peak for products whose fundamentals are close to the product frequency. The latter are the same products which tend to add in phase from repeater to repeater and thus dominate on long systems. These "significant" distortion products increase in power by about 6 dB between room and sea-bottom temperatures, while those which were measured during development and manufacture decrease about 1 dB over the same temperature range.

7.2.2 Source of excess third-order distortion

Because of the frequency, power level, and temperature dependence of repeater third-order distortion, the initial characterization was inadequate and misleading. Improved measurement techniques indicated that the two surge-protection diodes in the output network increased the repeater distortion by about 12 dB. Distortion caused by these diodes cannot be explained in terms of conventional behavior involving nonlinear resistance and capacitance. The distortion can, however, be explained semi-quantitatively in terms of nonlinear MOS (metal-oxide-semiconductor) capacitance and conductance effects. In addition, tests have shown that when the reverse-biased output network diodes are replaced with reverse-biased MOS capacitors, the resulting distortion contours have characteristics similar to those of Fig. 24. The distortion, while of third-order type, is actually produced by second-order interaction; second-order products are generated and modulated again with the fundamental signals. At the time of this writing, it is not clear in detail how the MOS-type nonlinearity is produced in the surge-protection diodes. Figure 25a is a block diagram of a nonlinear network whose calculated isomodulation contours have the same characteristics, Fig. 25b, as those measured on an SG repeater.

7.2.3 Future noise improvement on TAT-6

Following the successful analytical modeling of the repeater third-order distortion, an experimental post-distorter network was designed, built, and tested. The distorter, consisting of diodes and linear networks, achieved 15 to 20 dB of third-order distortion reduction on a single repeater over a 10-dB dynamic range.

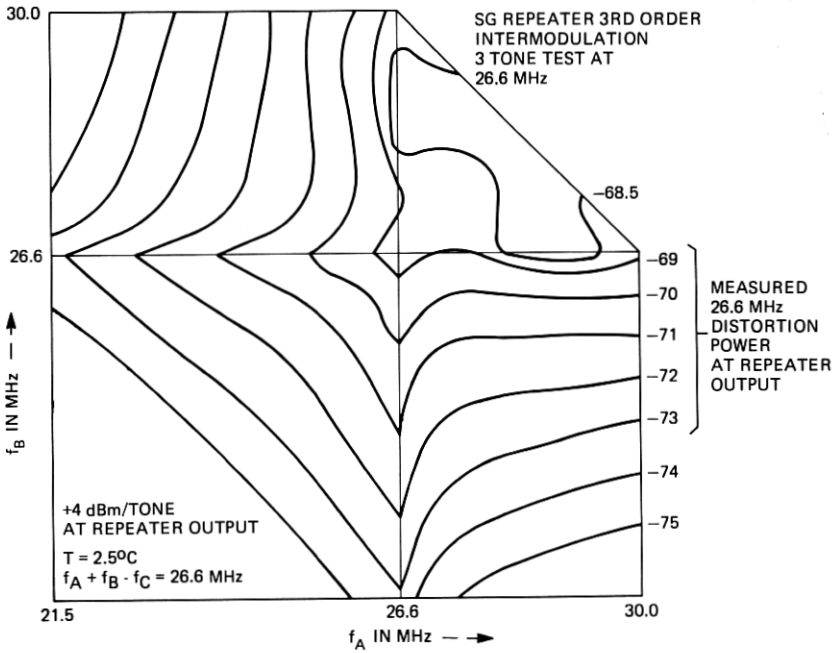

Fig. 24—Isomodulation contours of SG repeater with surge protection diodes.

It was further successfully tested as a possible noise canceler on TAT-6 by noise-loading single supergroups in the portion of the high band where delay distortion is relatively small.

A post-distorter is presently being constructed for the three top hypergroups of TAT-6. It consists of 34 tandem distorter networks connected by loss equalizers, phase equalizers, and amplifiers. Each distorter network will cancel the distortion produced by one block of 20 repeaters. A 13-dB suppression of third-order distortion is expected, which should reduce total noise by the 6 dB required to meet the original system design objectives. The loss equalizers in the post-distorter are adjustable to track the system loss change with time.

7.2.4 Noise improvement on future SG systems

Prior to completion of TAT-6, the design of the 82-type transistor had been modified to improve its ability to withstand surges. The new "double epitaxial" design features a two-step collector impurity profile which increases the collector-emitter breakdown voltage while maintaining exceptional linearity. This improvement allowed removal of the two surge-protection diodes in the output network and one gas tube in each GSF. Since the semiconductor diodes contributed nearly all the excess third-order intermodulation noise, most of the necessary im-

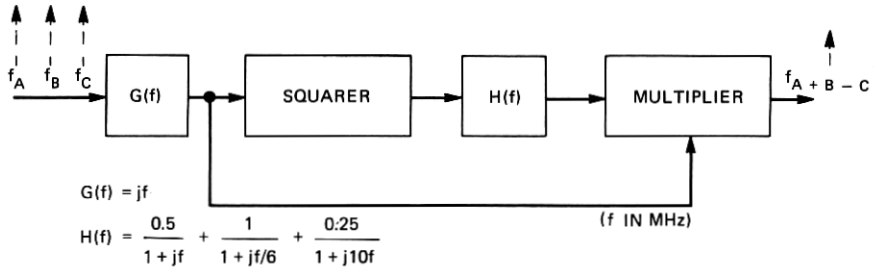

(a)

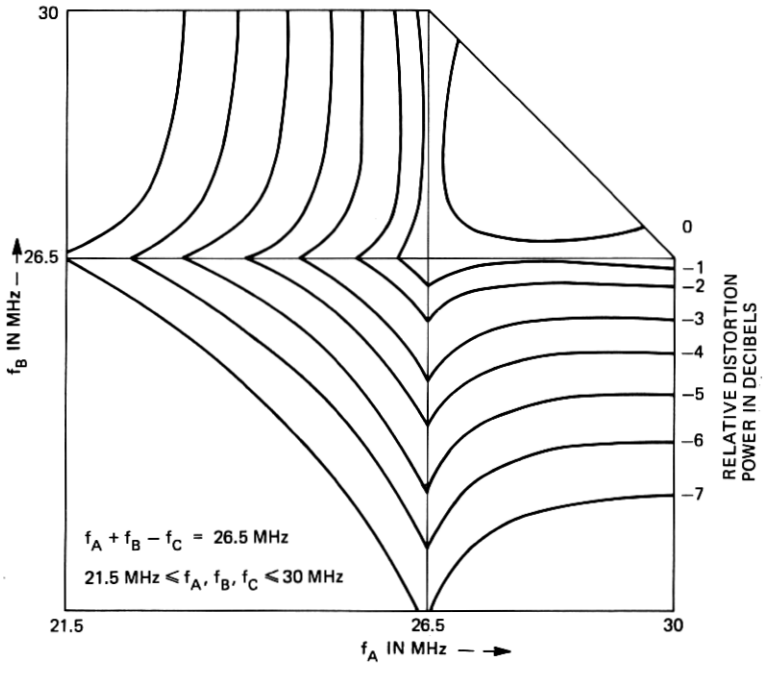

(b)

Fig. 25—(a) A fundamental frequency dependent third-order distorter. (b) Computed 26.5-MHz response of distorter.

provement in repeater linearity was achieved before the problem was discovered.

Further investigation of transistor third-order distortion revealed that it had two characteristics of the diode distortion, unusual power level and fundamental-frequency dependence. It was discovered that these characteristics could be essentially eliminated by changing the crystal orientation of the transistor from the ⟨111⟩ axis to the ⟨100⟩ axis. It

appears that the MOS capacitance associated with metallization and the oxide passivation layer is the source of the unusual distortion. Third-order distortion measurements ($A + B - C$ type products) on samples of MOS capacitors have shown that capacitors built on a ⟨111⟩ crystal orientation generate 13- to 17-dB more distortion than those built on ⟨100⟩ crystals. This difference in distortion is probably proportional to the difference in interface energy state densities for the two orientations.[10] Semiconductor distortion studies are being continued in an effort to more fully understand and characterize the physical mechanisms which produced this unforeseen behavior. The results of these studies will be published when they have been completed.

REFERENCES

1. "SF Submarine Cable System," B.S.T.J., *49*, No. 5 (May–June 1970), pp. 601–798.
2. S. T. Brewer, R. L. Easton, H. Soulier, and S. A. Taylor, "SG Undersea Cable System: Requirements and Performance," B.S.T.J., this issue, pp. 2319–2354.
3. G. E. Morse, S. Ayers, R. F. Gleason, and J. R. Stauffer, "SG Undersea Cable System: Cable and Coupling Design," B.S.T.J., this issue, pp. 2435–2469.
4. C. D. Anderson, "Overload Stability Problem in Submarine Cable Systems," B.S.T.J., *48*, No. 6 (July–August 1969), pp. 1853–1864.
5. M. Brouant, C. Chalhoub, P. Delage, D. N. Harper, H. Soulier, and R. L. Lynch, "SG Undersea Cable System: Terminal Transmission Equipment," B.S.T.J., this issue, pp. 2471–2496.
6. W. M. Fox, W. H. Yocum, P. R. Munk, and E. L. Sartori, "SG Undersea Cable System: "Semiconductor Devices and Passive Components," B.S.T.J., this issue, pp. 2405–2434.
7. J. V. Milos and P. A. Yeisley, "Manufacturing Aluminum Castings and Extrusions for use in SG Submarine Cable Repeaters," Western Electric Engineer, July 1975.
8. A. T. Chapman et al., "Manufacture of Submarine Cable Repeaters and Ocean Block Equalizers," B.S.T.J., *49*, No. 5 (May–June 1970), pp. 663–681.
9. W. J. Geldart, et al., "A 50 Hz–250 mHz Computer-Operated Transmission Measuring Set," B.S.T.J., *48*, No. 5 (May–June 1969), pp. 1339–1381.
10. P. V. Gray and D. M. Brown, "Density of SiO_2-Si Interface States," Appl. Phys. Lett., 8 (1966), pp. 31–33.